Tuning Singlet Fission in π-Bridge-π Chromophores

Elango Kumarasamy,[1,‡] Samuel N. Sanders,[1,‡] Murad J. Y. Tayebjee,[2,3] Amir Asadpoordarvish,[4] Timothy J.H. Hele,[5,6] Eric G. Fuemmeler,[5] Andrew B. Pun,[1] Lauren M. Yablon,[1] Jonathan Z Low,[1] Daniel W. Paley,[1,7] Jacob C. Dean,[8] Bonnie Choi,[1] Gregory D. Scholes,[8] Michael L. Steigerwald,[1] Nandini Ananth,[5] Dane R. McCamey,*[4] Matthew Y. Sfeir,*[9] and Luis M. Campos*[1]

[1]Department of Chemistry, Columbia University, New York, New York 10027, USA

[2]School of Photovoltaic and Renewable Energy Engineering, University of New South Wales, Sydney NSW 2052, Australia

[3]Cavendish Laboratory, University of Cambridge, J.J. Thomson Avenue, Cambridge CB3 0HE, UK.

[4]ARC Centre of Excellence in Exciton Science, School of Physics, University of New South Wales, Sydney, NSW 2052, Australia

[5]Department of Chemistry and Chemical Biology, Cornell University, Ithaca, NY 14850, USA

[6]On intermission from Jesus College, Cambridge University, UK

[7]Columbia Nano Initiative, Columbia University, New York, NY, 10027, USA

[8]Department of Chemistry, Princeton University, Princeton, NJ 08544, USA

[9]Center for Functional Nanomaterials, Brookhaven National, Laboratory, Upton, New York 11973, USA

Table of Contents

1. Transient Absorption and Triplet Photosensitization Experiments

Details of the transient absorption experiments have been described previously.[1,6,16] Briefly, a 1 kHz amplified Ti:Sapphire system equipped with an optical parametric amplifier is used to generate resonant pump pulses with a pulse width of ~ 100 fs. This laser is also used to generate a femtosecond supercontinuum probe in a thin sapphire plate that is mechanically delayed with respect to the pump pulse. A nanosecond supercontinuum probe pulse generated in a fiber laser (Leukos) is alternately employed using an electronically delayed configuration to investigate longer delayed times. The pump pulse is the same for both probe configurations. The measurements are conducted at concentrations below 100 μM, and typically ~50 μM in bipentacene unless otherwise noted.

Triplet photosensitization measurements were performed to ascertain the spectrum and lifetime of individual triplets in these systems. In these measurements, ~20 mM of anthracene is dissolved in chloroform along with <100 μM bipentacene. Photoexcitation of the anthracene at 360 nm (~100 μJ/cm^2), followed by intersystem crossing and collisions with bipentacenes results in population of individual triplets in the pentacene molecules of interest. This process can be seen as the photoinduced absorption (PIA) from the anthracene triplet, most prominent near 420 nm, decays; while the pentacene triplet PIA, most prominent near 520 nm, rise in each case (Figure S1).

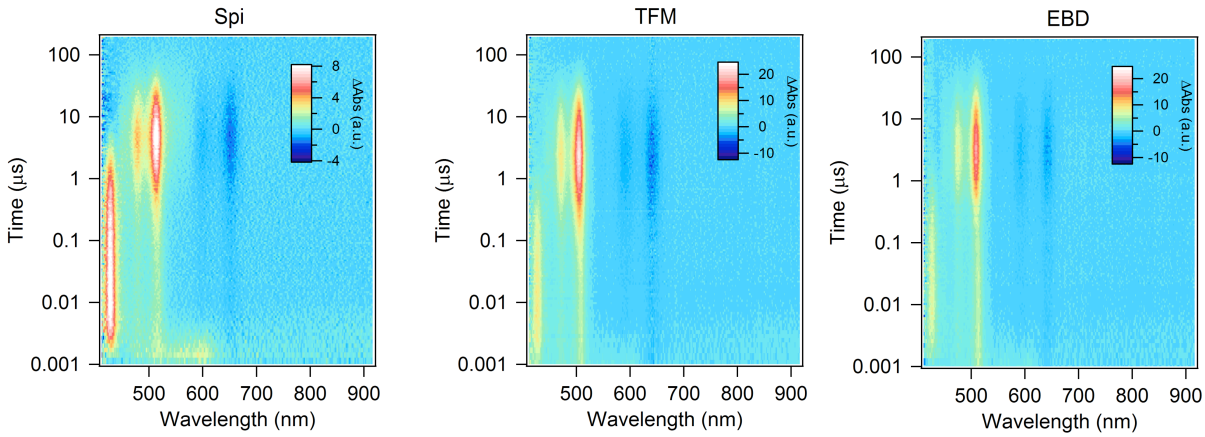

Figure S1: Triplet photosensitization measurements of bipentacene (~50 µM) and ~20 mM anthracene dissolved in chloroform, with excitation at 360 nm (~100 µJ/cm^2) preferentially exciting anthracene molecules. Color scale is reported in arbitrary units.

If we examine the spectrum of the PIA after sufficient time has passed, so that only pentacene triplets remain, we can ascertain the spectrum of an individual pentacene triplet in these systems. We can then compare this spectrum to spectrum produced by direct photoexcitation, which we expect to produce triplet pairs if singlet fission is operative. Shown below in Figure S2, these comparisons confirm that the state produced by direct photoexcitation of the bipentacenes (orange traces) can be assigned as triplet excitons. We note that some modest discrepancies are expected, as interactions between the two triplets in a pair can perturb the spectrum relative to that of individual triplets populated in sensitization experiments.[1,2]

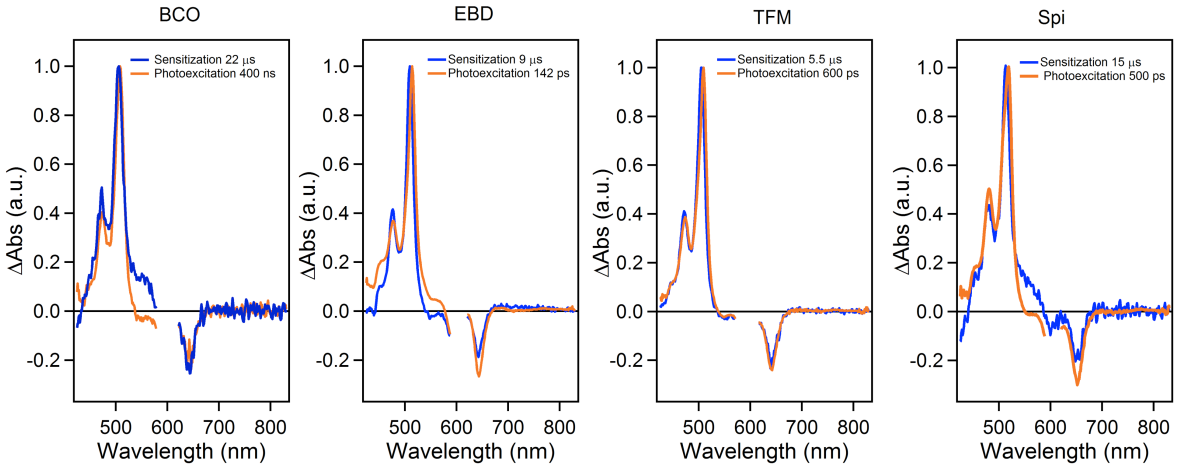

Figure S2: Comparison of spectral shape produced by photoexcitation (orange traces, triplet pair spectra) versus photosensitization (blue traces, individual triplet spectra), with each trace normalized to the maximum value.

1.1. Sensitization Yield Determination for BCO

The same sensitization experiments were performed for **BCO**. However, in this case, we have undertaken further, quantitative measurements of PIA produced by photoexcitation to also determine a cross-sectional triplet yield for this compound. This process is explained in detail below.

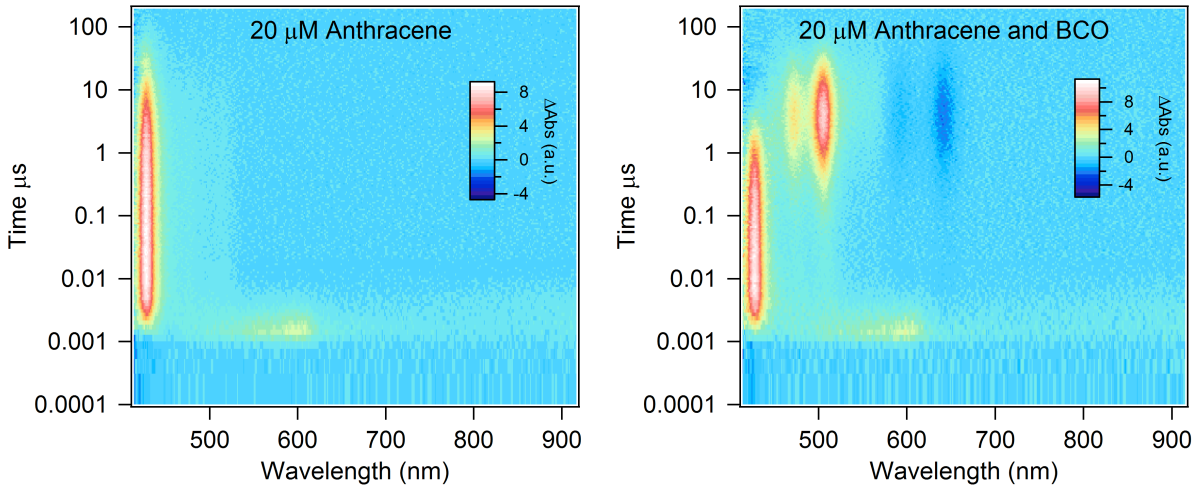

Figure S3: Photosensitization measurements for **BCO**, sensitized by ~20 mM anthracene in chloroform by the same procedure described above, where the color scale is in units of mOD.

Raw 2D color plots of sensitization experiments used to determine the triplet absorptivity for **BCO**. The intrinsic lifetime of the 20 μM anthracene solution is found to be ~45 μs. In the presence of the **BCO**, the lifetime was truncated to ~1.96 μs, giving a transfer efficiency of 92.3%. Comparing the ratio of triplet absorption at the λ_{max} for anthracene, known as 55,200, to the triplet absorption of the **BCO** ~507nm, and accounting for decay of **BCO** triplet signal during transfer (23 μs triplet lifetime), we find the molar absorptivity of the **BCO** triplet:

$$\varepsilon_{T-T}(BCOBP) = \frac{0.00951}{0.01081} * 55200 * \frac{1}{.959} * \frac{1}{.923} = 54{,}862 M^{-1} cm^{-1}$$

Solution	O.D. at 600 nm	(1-T) at 600 nm	$M^{-1}cm^{-1}$
TIPS Pentacene	0.2873	0.48	21000
BCO	0.3653	0.57	47000

The concentration of singlets in the TIPS pentacene sample is estimated from the maximum of the GSB signal of -0.0018187, as well as the molar absorptivity and cuvette length, as shown below.

$$Concentration\,(TIPS\ pent\ singlet) = \frac{-0.0018187}{21000 * 0.1} = 8.66 * 10^{-7} M$$

The singlet concentration for the **BCO** sample is then found under the same excitation conditions by simply comparing the number of photons absorbed:

$$Concentration\,(BCO\ singlet) = 8.66 * 10^{-7} * \frac{57}{48} = 1.03 * 10^{-6} M$$

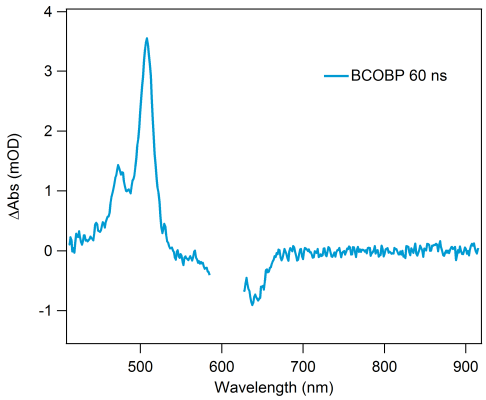

Figure S4: Photoinduced absorption in chloroform for **BCO** at 60 ns, used for yield calculation

The triplet concentration can be found using the following relationship:

$$Triplet\ concentration = \frac{\Delta A}{\varepsilon_{T-T} * l} = \frac{.00355}{54862 * .1} = 6.47 * 10^{-7} M$$

Comparing the triplet concentration at 60 ns (Figure S4), after singlet decay is complete, but triplet decay has not substantially occurred, we find the triplet yield:

$$Yield\,(triplets) = \frac{6.47 * 10^{-7}}{1.03 * 10^{-6}} = 0.63$$

The triplet yield of 63 % is consistent with a simple kinetic argument. The intrinsic lifetime of TIPS pentacene in chloroform is 12.3 ns. The singlet in **BCO** decays with a monoexponential 7.6 ns lifetime. Assuming dimer has similar intrinsic dynamics to monomer, we can estimate a singlet fission rate and yield from the reduction in singlet lifetime:

$$\frac{1}{7.6\,ns} = \frac{1}{12.3} + \frac{1}{SF\ time\ constant}$$

SF time constant is therefore approximated as 20 ns. Competition between a 20 ns process (singlet fission) and a 12.3 ns process (radiative and non-radiative monomer decay) predicts:

$$\frac{12.3}{12.3 + 20} = 0.38$$

Based on these kinetics, we should expect 38% of the singlet excitons to undergo SF. Therefore, we expect a ~76% triplet yield if SF is the only triplet formation mechanism. The yield determined by sensitization of 63% agrees well with a SF dominated mechanism for triplet formation, and is much too high to be explained by intersystem crossing (in which case only 38% triplet yield would be expected). The slightly lower actual triplet yield could be explained by a small contribution to triplet formation from ISC, but the expected 76% yield is certainly within the margin of error for the triplet yield calculations. The significant contributions from SF are also unambiguously characterized by the population of triplet pair states observed in tr-ESR experiments, described in the main text.

In Figure S5 is the UV-vis reproduced from the main text, but with units of molar absorptivity.

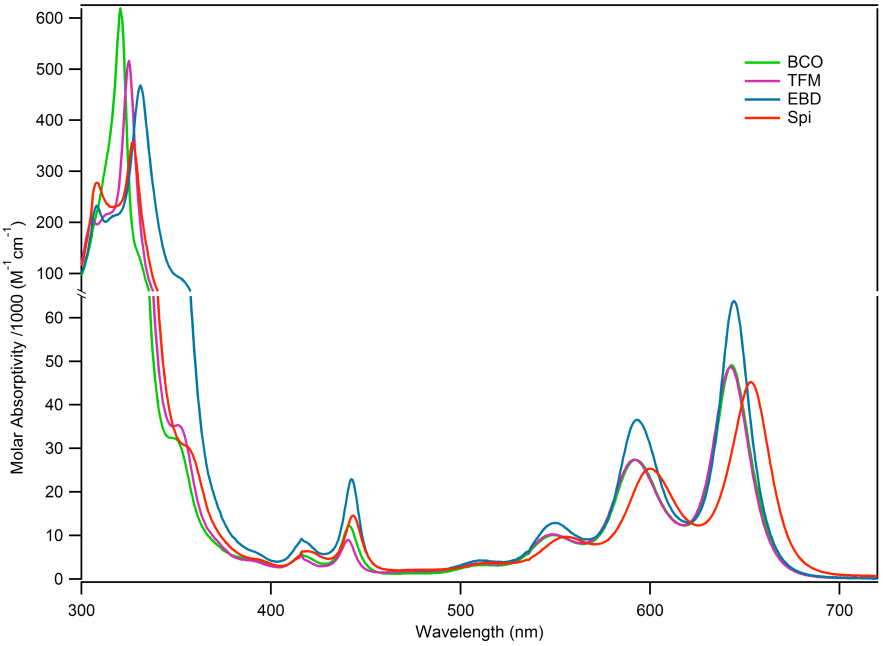

Figure S5: UV-visible absorption spectra for the pentacene dimers investigated in this manuscript in units of molar absorptivity

In general, the absorptivity for the dimers is approximately twice that of the TIPS pentacene monomer (~20,000 $M^{-1}cm^{-1}$) near the absorption maximum ~650 nm.

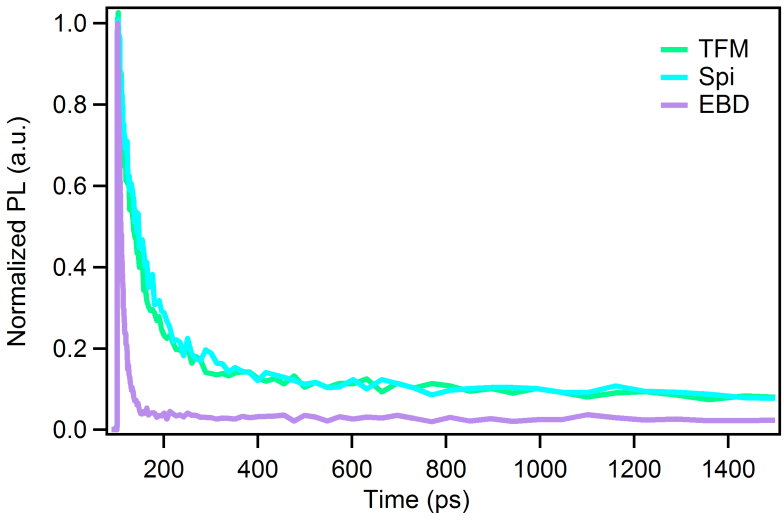

Figure S6: Decay of photoluminescence for ~50 μM solutions in chloroform, monitored at 680 nm after photoexcitation at 600 nm (~50μj/cm^2)

Upconverted photoluminescence as a function of time is shown in Figure S6 for excitation in chloroform at 600 nm and monitoring at 680 nm. The singlet decay is correlated well with the singlet

decay time constants found in transient absorption spectroscopy. Some residual PL, most notable in **TFM** and **Spi**, has a lifetime of ~12 ns and is attributed to monomeric pentacene impurity emission.

1.2. Solvent Dependence on Singlet Fission Rate for Spi

Below in Figure S7, we plot the rates of singlet fission for the pentacene dimers studied in this manuscript as a function of solvent. These rate assignments are achieved by modeling transient absorption data using global analysis in the program Glotaran.[3] The two dimensional color plots, showing induced absorption as a function of time and wavelength, which are inputted to determine singlet fission rate constants, are shown below for the different dimers and solvents.

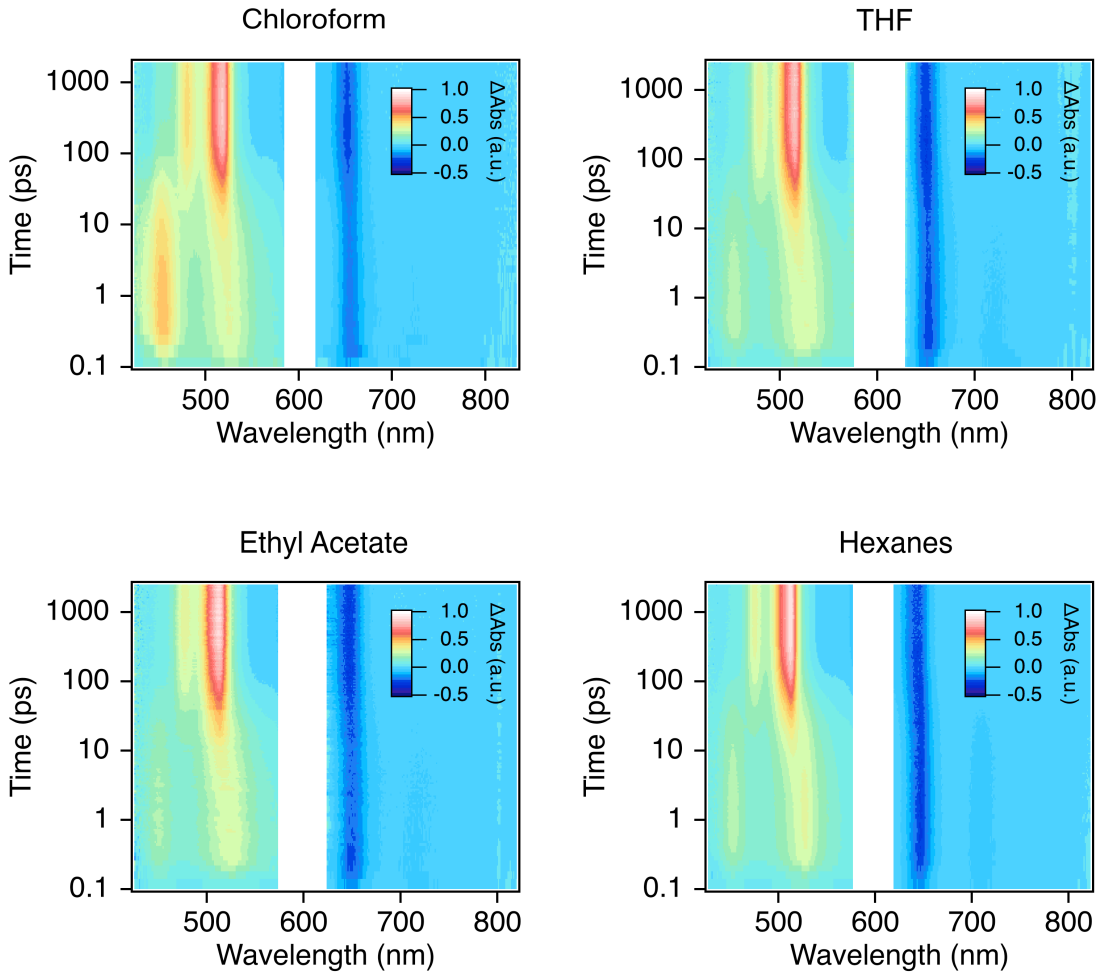

Figure S7: Transient absorption data of **Spi** in different solvents, with excitation at 600 nm (~50μj/cm^2).

1.3. Solvent Dependence on Singlet Fission Rate for BCO

Shown below in Figure S8 are the transient absorption color plots for **BCO** in different solvents. These data were recorded using an electronically controlled delay between pulse and probe. While the ~0.5 ns time resolution of this technique results in relatively poor time resolution near time 0, it is sufficient to assign the >7 ns time constants for singlet fission in this system.

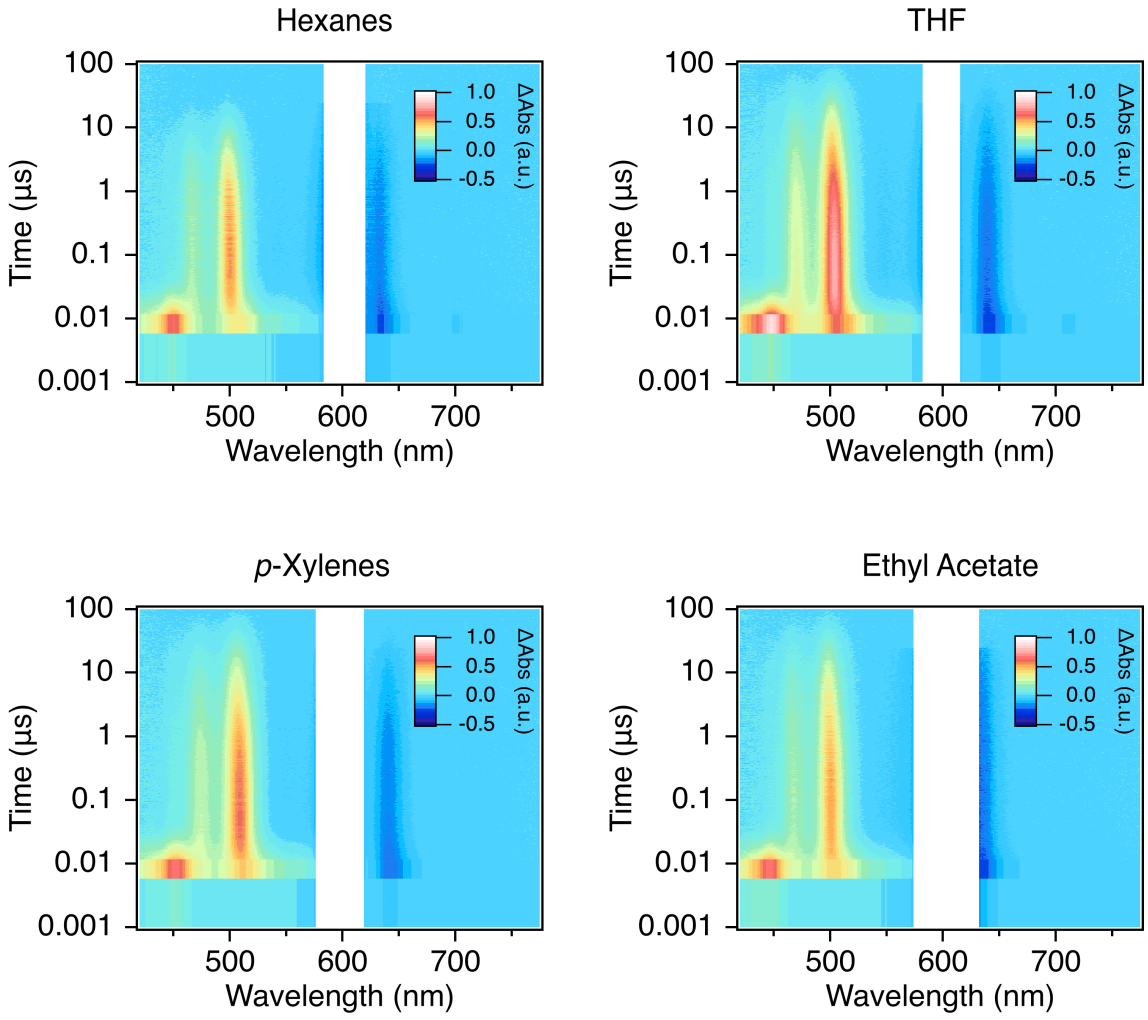

Figure S8: Transient absorption data of **BCO** in different solvents, with excitation at 600 nm (~50µj/cm^2). The instrument response is approximately 0.5 ns while singlet decay ranges from about 7–11 ns, making the dynamics sufficiently resolved for assignment of accurate rate constants

1.4. Solvent Dependence on Singlet Fission Rate for EBD

Shown below in Figure S9 are transient absorption spectra for **EBD** in different solvents.

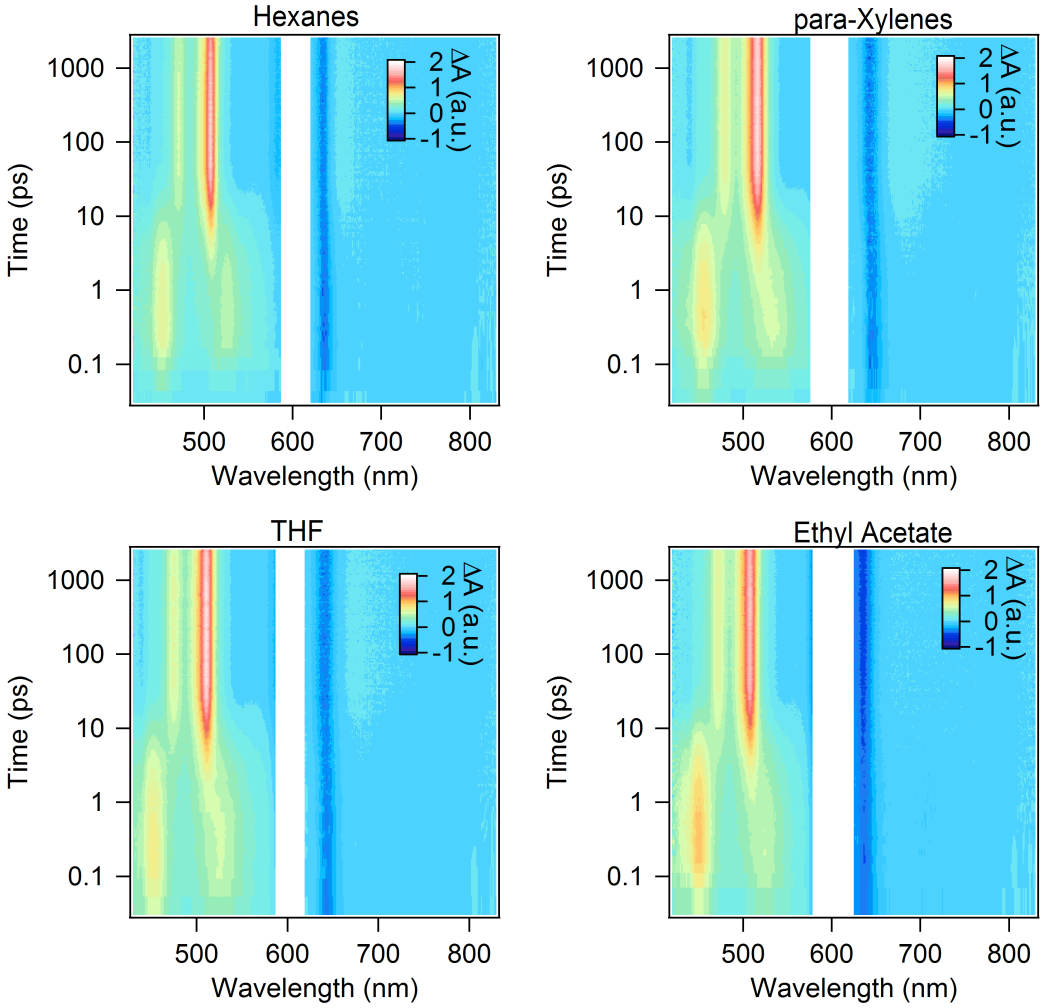

Figure S9: Transient absorption spectra of **EBD** in different solvents, with excitation at 600 nm (~50μj/cm^2).

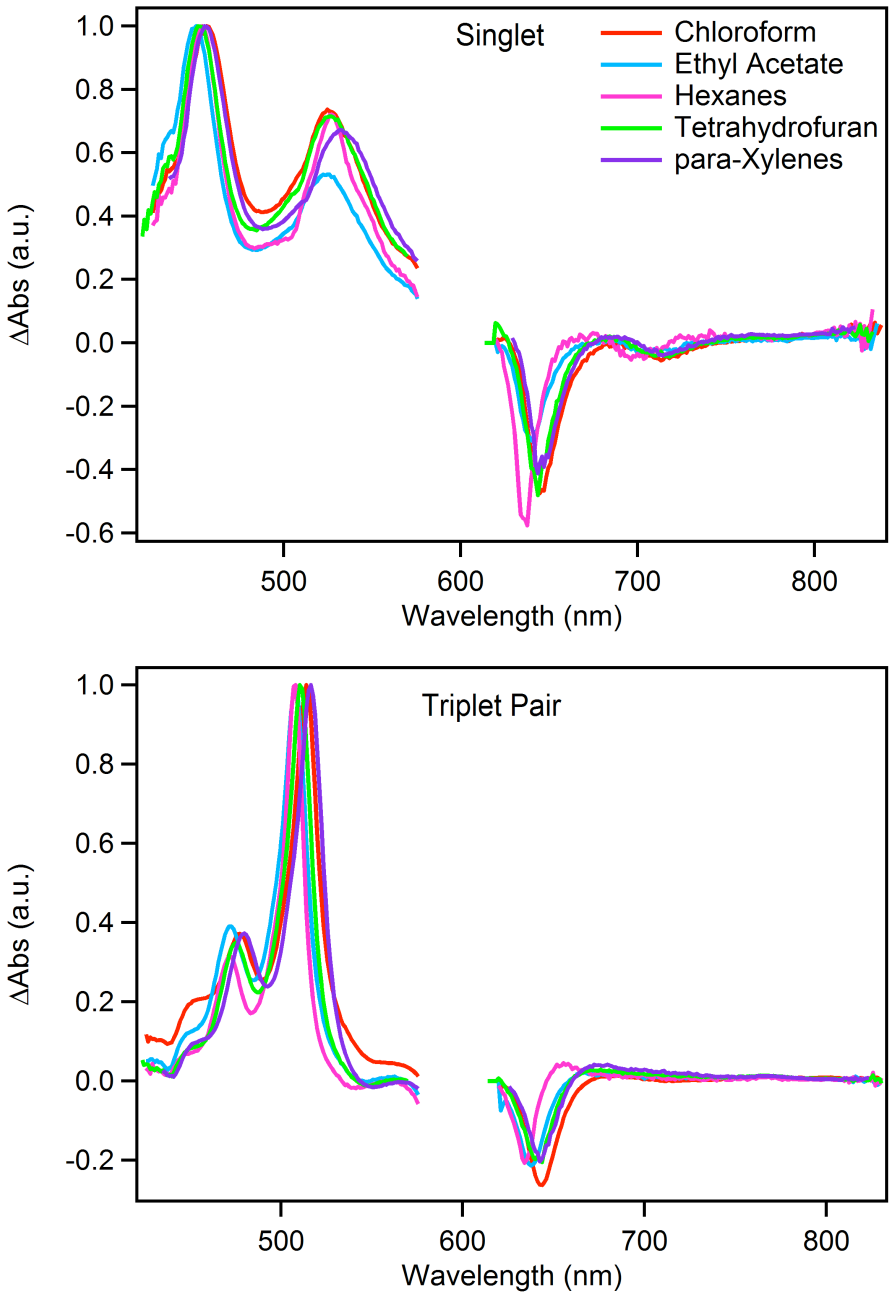

Figure S10: Transient spectra of the singlet and triplet pair of **EBD** in different solvents, derived from a global analysis sequential decay model.

1.5. Solvent Dependence on Singlet Fission Rate for TFM

Shown in Figure S11 are the transient absorption spectra for **TFM** in different solvents. These data sets were used to determine singlet fission rates, given in the main text.

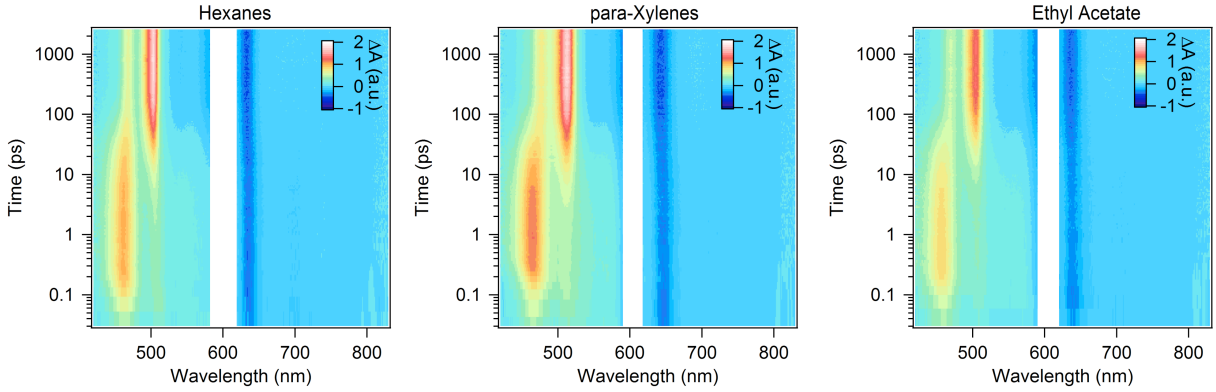

Figure S11: Transient absorption data for **TFM** in different solvents with excitation at 600 nm (~50μj/cm^2).

1.6. Global Analysis: Spectra and Time Constants

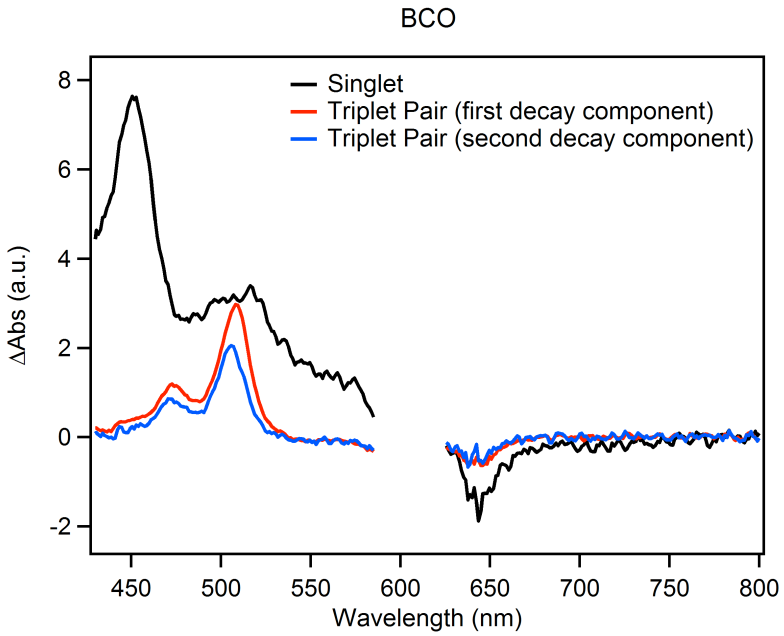

FIGURE S12: Spectra isolated from global analysis of longer-timescale, electronically controlled delay data for **BCO** in chloroform from 600 nm, ~50μJ/CM^2 excitation.

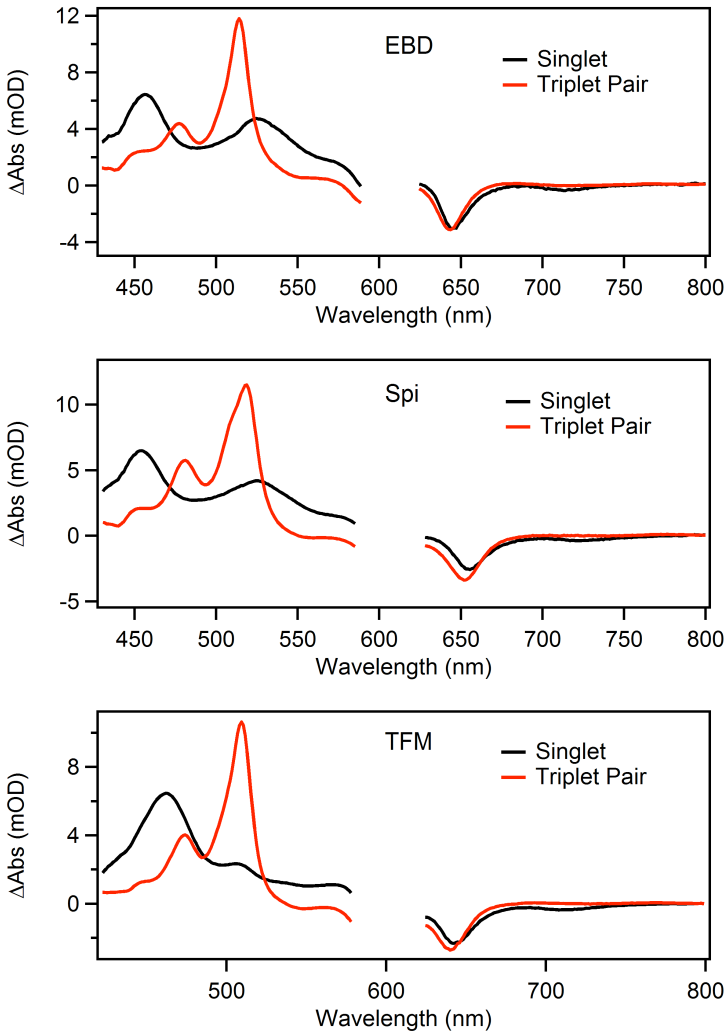

FIGURE S13: Spectra isolated from global analysis of ultrafast transient absorption data (first ~2.7 ns, mechanically controlled delay) for the singlet and triplet pair in chloroform.

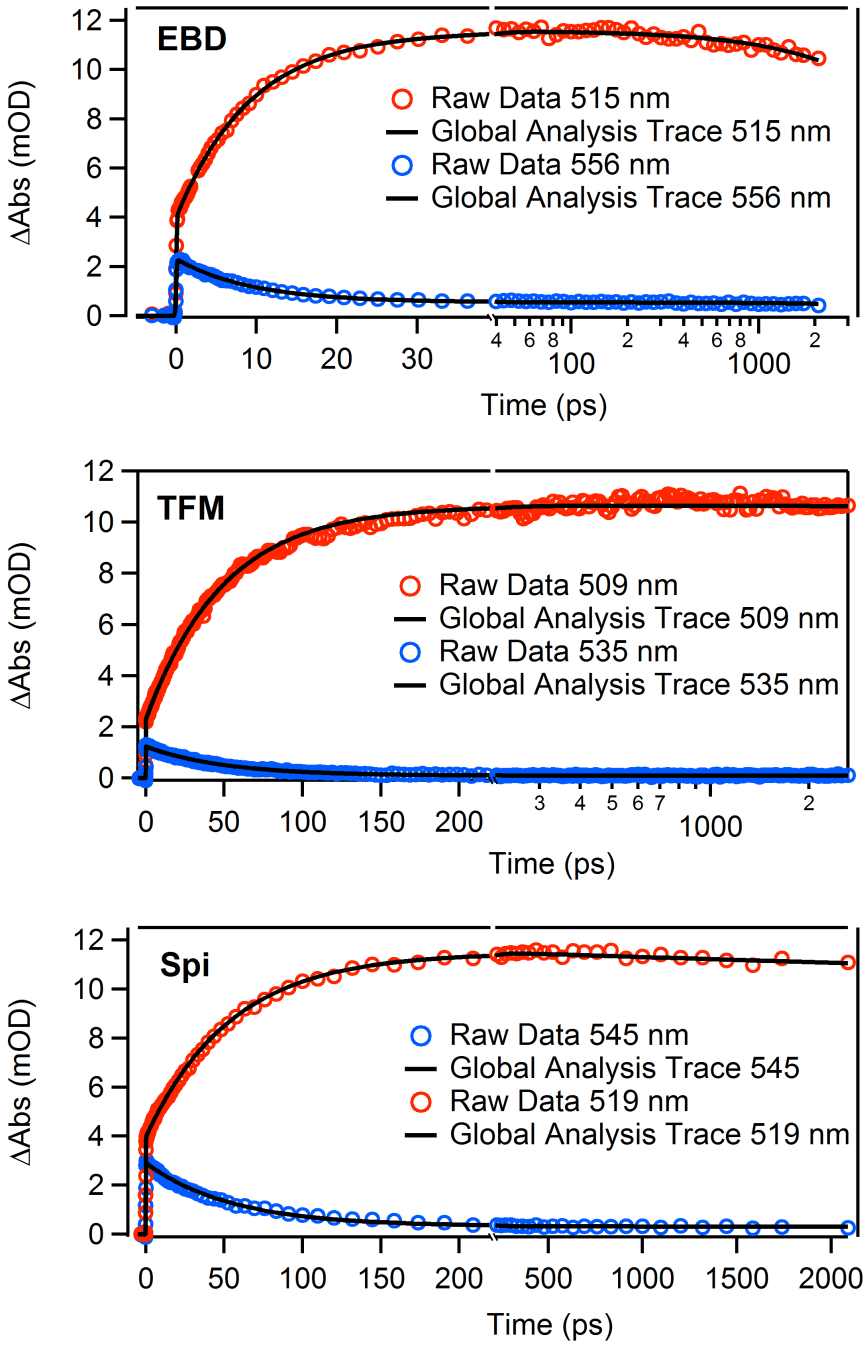

FIGURE S14: Comparison of kinetic cuts through the raw transient absorption data (chloroform as solvent) to the fits derived from a sequential decay model of the singlet into a triplet pair. The corresponding 2D color plots from which these cuts are derived are found in the main text.

1.7. Solvent Dependence of Singlet Fission and Triplet Pair Recombination for BCO

Shown in Figure S11 are the time constants for singlet fission in **BCO** as a function of solvent. Like the homoconjugated pentacene dimers in the main text, there is no clear trend with solvent polarizability. However, there is a modest trend towards faster singlet fission rates in more polar solvents. However, as shown on the right, triplet pair recombination time constants, given by the first exponent for triplet recombination in **BCO**, also accelerate in more polar solvents. The similarity of these trends points towards a more mundane explanation for these modest trends in these systems with large pentacene center-to-center distances, where CT states are high above the singlet state. The modest trend here is unlikely to necessitate mediation by virtual charge transfer states, as these states are not, to our knowledge, implicated in enhancing triplet pair recombination rates. Whether the modest rate enhancements over massive polarity ranges reported here are due to geometric differences in solvents of different polarities, differences in solvent reorganization energies, or other factors is still an open question. Regardless, it seems that the direct mechanism is dominant for this series of molecules.

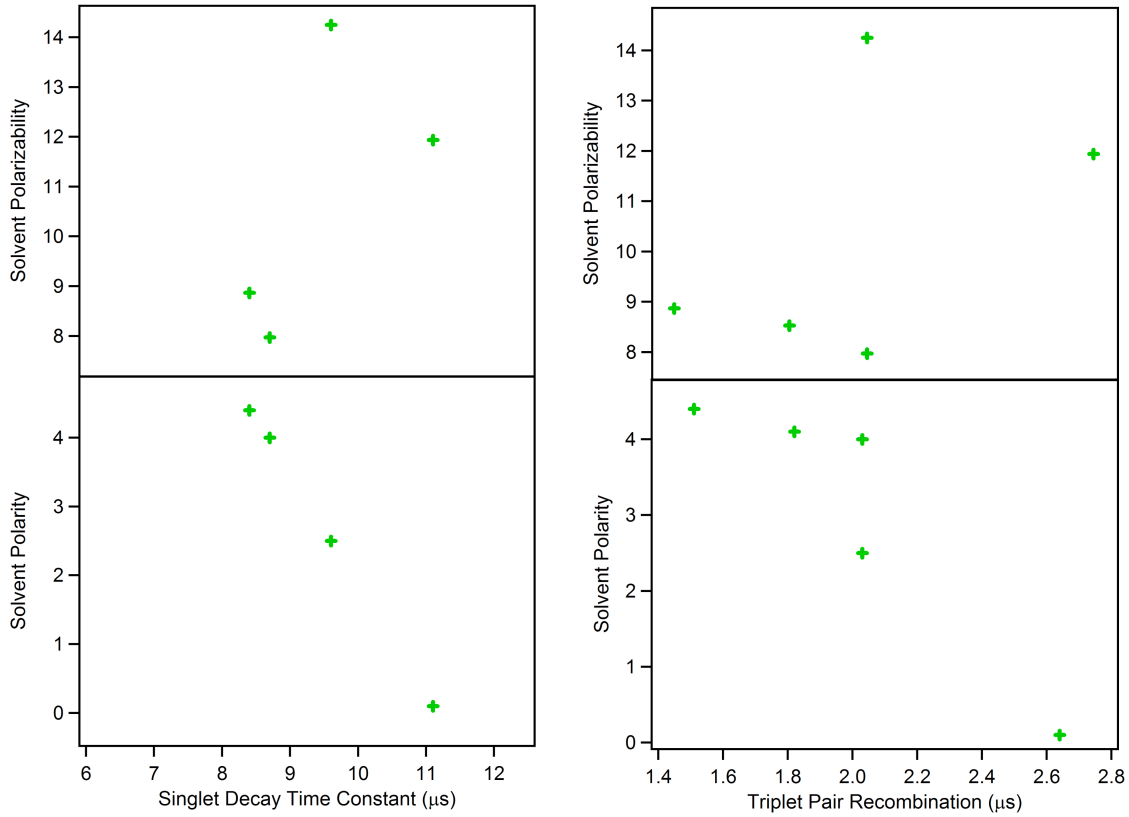

Figure S15: Time constants of singlet decay and triplet pair recombination for **BCO** as a function of solvent polarity (P') and polarizability (α). The polarity[4] and polarizability[5] values respectively, for hexanes (0.1, 11.94), p-xylenes (2.5, 14.25), chloroform (4.1, 8.53), tetrahydrofuran (4.0, 7.97), ethyl acetate (4.4, 8.87).

1.8. Solvent Dependence of Singlet Fission of TFM, Spi and EBD

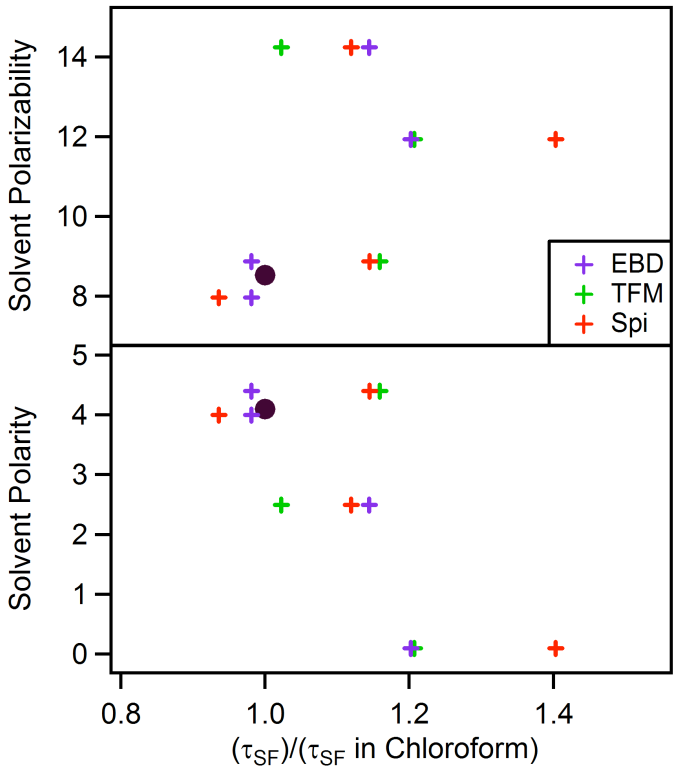

Figure S16: Singlet fission time constants, normalized to the time constant in chloroform, as a function of solvent polarity (P') or polarizability (α)

TABLE S1: Summary of time constants in picoseconds for singlet fission (or singlet decay in the case of **BCO**) of dimers in different solvents.

	Hexanes	***p*-Xylenes**	**THF**	**Chloroform**	**Ethyl acetate**
EBD	12.5 ps	11.9 ps	10.2 ps	10.4 ps	10.2 ps
TFM	60 ps	50.8 ps	n/a	49.7 ps	57.6 ps
Spi	76.5 ps	61 ps	51 ps	54.5 ps	62.4 ps
BCO	11000 ps	9600 ps	8700 ps	7600 ps	8400 ps

TABLE S2: Summary of time constants in microseconds for triplet pair recombination of dimers in different solvents.

	Hexanes	***p*-Xylenes**	**THF**	**Chloroform**	**Ethyl acetate**
BCO	2.64 µs	2.03 µs	2.03 µs	1.82 µs	1.51 µs

1.9. Fluence Independent Dynamics in BCO

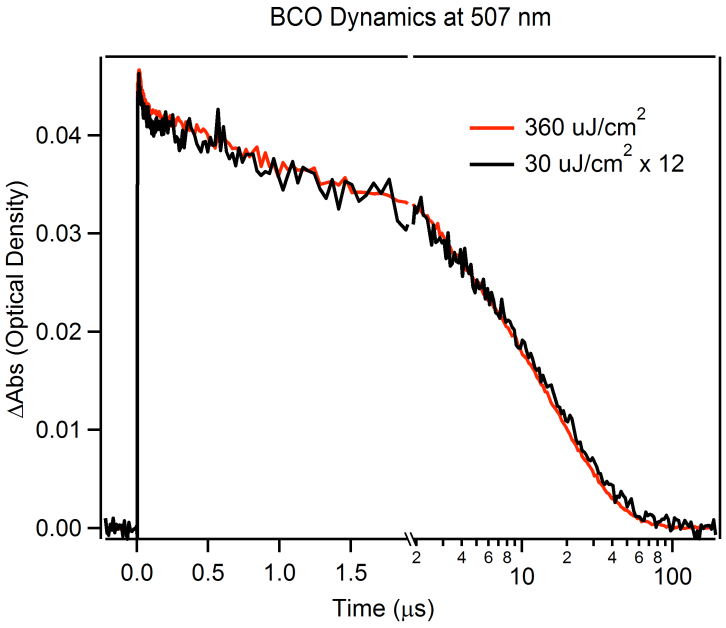

Figure S17. Kinetic Traces at 507 nm for low (30 µJ/cm^2) and high (360 µJ/cm^2) pump fluence reveal fluence independent dynamics.

2. ELECTRONIC STRUCTURE THEORY: GENERAL METHODS

In accordance with previous work the Si(iPr$_3$) groups were replaced with Hydrogens as they do not substantially affect the electronic structure.[6] All calculations used the GAMESS-US package[7], some of which were run on XSEDE resources.[8]

Structural optimization was undertaken using density functional theory (DFT) with the B3LYP functional and a 6-31G* basis. To accelerate convergence of the optimization a Hessian was initially obtained at the restricted Hartree-Fock (RHF) level using a SBKJC pseudopotential basis, and used to initialize the DFT calculation.

The **TFM**, **Spi**, and **BCO** structures were optimized in the C_2 point group, **BP1** in the C_i point group and **EBD** in the C_{2v} point group.

Due to the large size and high computational cost, multiconfigurational calculations used an SBKJC basis with *d* functions on carbon and fluorine (if present) added from the 6-31G* basis set. This has previously been demonstrated as being sufficient for an accurate description of the excited states of pentacene and its dimers[6,9].

CASSCF calculations used a RHF reference and were state-averaged over singlet states with equal weights. For **TFM**, **Spi** and **BCO** the state averaging was over the lowest four states of A symmetry and the lowest four states of B symmetry. For **BP1** this was over the lowest four states of A_g symmetry and the lowest four states of A_u symmetry. For **EBD**, state averaging was over the lowest two singlet states of A_1, A_2, B_1 and B_2 point groups. The number of configuration interaction states to be found by the CASSCF calculation was adjusted on a case-by-case basis in order to include as many singlet states as were requested (since triplet and quintet states were also included in the configuration interaction states).

The CASSCF calculations all used a four orbital, four electron (4o4e) active space comprising the HOMO-1, HOMO, LUMO and LUMO+1 of the dimer. Previous research has shown that for quantitative accuracy an 8o8e active space (or larger) may be necessary for accurate excitation energies, though diabatizing the resulting states or assigning their character can be challenging.[6,9] Preliminary calculations with 8o8e active spaces on these molecules, which due to the linkers are larger than the pentacene dimers previously studied by these methods, were found to be unfeasible on the grounds of computational cost and numerical instability. We therefore consider 4o4e calculations, whose excitation energies are only qualitatively accurate, but whose character can be clearly described as excitonic, charge-resonance and multiexciton (see below).[10]

For accurate excitation energies, second order perturbation theory (MRMP) was applied using multiconfigurational quasidegenerate perturbation theory (MCQDPT) with the standard intruder state avoidance parameter of 0.02 E_h^2.[9]

In accordance with previous research, we assign the character of: ground state (GS); local (intra-monomer) exciton (EX); charge-resonance states (CR), sometimes referred to as charge-transfer; and multiexciton (triplet-triplet with zero overall spin) (ME).[10] States with character of a double excitation within a monomer (sometimes referred to as “dg” or “gd”) can be used for inferring the relative signs of orbitals, but are otherwise not considered further.

GS and ME always transform as the totally symmetric representation, whereas EX and CR states commonly arise as symmetric and antisymmetric pairs. Here we consider only the antisymmetric EX and CR states, since in general only the antisymmetric pair is bright (has a substantial dipole moment from the ground state, as can be inferred from symmetry arguments), and it is expected that this will couple to the

antisymmetric CR state (since the nuclear kinetic energy operator is totally symmetric). In practice, the weak coupling in these systems means that the symmetric and antisymmetric pairs are expected to be of very similar energy.

To summarize, the point groups and irreps used are:

Point group	**C_2**	**C_i**	**C_{2v}**
Associated molecules	**TFM**, **Spi**, **BCO**	**BP1**	**EBD**
GS and ME symmetry	A	A_g	A_1
EX and CR symmetry	B	A_u	B_2

To assign the character of the excitations we use the dimer molecular orbitals linear combination of fragment orbitals (DMO-LCFMO) procedure,[11] which has previously been used to describe singlet fission.[10] In brief, this involves writing out the linear combination of determinants of the states we wish to describe in the monomer basis (suitably symmetry-adapted to spin and point group) and transforming to dimer orbitals, leading to a configuration interaction (CI) expansion in the basis of dimer orbitals. By the symmetry of the molecules (see above) the dimer orbitals must be either in-phase or out-of-phase combinations of monomer orbitals (such as A or B in the C_2 point group), and we make the small additional assumption that the dimer HOMO and HOMO-1 are well-described as in-phase and out-of-phase combinations of the monomer HOMOs only (not mixing in other monomer orbitals), and similarly for the dimer LUMO and LUMO+1. This is expected to be a good approximation in weakly coupled dimers such as those investigated in this article.

We then match the resulting CI expansions against the adiabatic states produced by the electronic structure theory calculations (in this case the CASSCF states which are then perturbed with MCQDPT) to assign the character of the state. In cases where different characters have the same linear combination of determinants except for a relative sign, such as EX and CR, we infer the relative signs of the orbitals from the CI expansion of the ME state and/or doubly excited states. For the B_2 irrep in **EBD** where there is no accessible symmetry-allowed state for comparison, the state closest in energy to the experimental bright excitation is assigned as EX.

We stress that this is not a localization or (quasi)diabatization calculation; the adiabatic states are not transformed, merely assigned to given ‘characters’. Excitations are assigned as follows:

Excitation energy (eV)	**EBD**	**TFM**	**Spi**	**BCO**	**BP1**
Local excitation (EX)	1.95	1.69	1.62	1.70	1.66
Multiexciton (ME)	2.42	1.68	1.59	1.69	1.64
Charge-resonance (CR)	3.11	2.89	2.73	3.27	3.10

For all pentacene dimers the CR state is over 1eV higher in energy than EX. All the states for **EBD** are anomalously high in energy (particularly ME) and we expect this is due to the higher symmetry (see above) such that fewer determinants can be used to variationally optimize a given CI expansion.

The high energy of the CR states is probably attributable to the spatial separation of the monomers (see Fig 2 of the main text) and the consequential Coulombic penalty to separating charges. Except for the anomalous **EBD** results, the simple Coulombic explanation is supported by the energy of the CR state increasing as the monomers are pushed further apart by the linker (see Fig 2), and in the case of **BCO** and **BP1** which have a similar spatial orientation, as the through-bond coupling between the monomers decreases:

E_{CT}(**Spi**)< E_{CT}(**TFM**) < E_{CT}(**BP1**) < E_{CT}(**BCO**).

Although these results are only qualitative and do not rule out a SF mechanism mediated by charge resonance (or other) states, they open the possibility of a direct pathway, consistent with earlier findings that singlet fission in bipentacenes occurs via a direct mechanism mediated by vibronic coupling.[6]

3. SINGLE CRYSTAL X-RAY DIFFRACTION

Data for pentacene dimers **TFM** and **BCO** were collected on an Agilent SuperNova diffractometer using mirror-monochromated Cu Kα radiation. Data collection, integration, scaling (ABSPACK) and absorption correction (face-indexed Gaussian integration[12] or numeric analytical methods[13]) were performed in CrysAlisPro. Structure solution was performed using ShelXT. Subsequent refinement was performed by full-matrix least-squares on F^2 in ShelXL.[14] Olex2[15] was used for viewing and to prepare CIF files. ORTEP graphics were prepared in CrystalMaker. Thermal ellipsoids are rendered at the 50% probability level.

3.1. Crystal structure of BCO:

The structure solved readily in P-1 with one molecule in the asymmetric unit. The ethylene bridges of the **BCO** moiety were disordered by a 180 deg. rotation about the bridgehead-bridgehead axis. The two disordered components were located in difference maps and refined with standard similarity and rigid-bond restraints.

The four independent Si(*i*-Pr)$_3$ groups were all disordered over two or three positions. A packing diagram showed that the minor positions of each group would collide with the major position of a different group, so therefore the disorder was modeled with a single free variable for the occupancies of all four independent silyl groups. One isopropyl group was disordered over three positions, which were modeled with the use of a SUMP restraint for the total site occupancy. Every independent position of a silyl group was made equivalent with a SAME instruction (a total of 9 equivalent silyl groups, since 3 were disordered over 2 positions and 1 was disordered over 3 positions.) All atoms were refined anisotropically with the disordered atoms stabilized by a RIGU restraint and a short-range SIMU restraint for overlapping ADPs. Hydrogen atoms were placed in calculated positions and refined with riding isotropic ADPs and coordinates.

3.2. Crystal structure of TFM:

The structure initially appeared to be ordered in C2/c, crystallizing on a twofold axis with ½ molecule in the asymmetric unit. The refinement of this model proceeded to R1 ~10% but suffered from large, unusual anisotropic ADPs for many atoms in the pentacene core. When these sites were split, the ratio of disordered components refined to 1:1, which suggested a possible special-position disorder generated by the twofold axis. Half of the split sites were transformed by the twofold axis, giving a model with 1 molecule in the asymmetric unit, and the whole molecule was placed in PART -1. When the two pentacene halves were restrained with a SAME instruction, the refinement proceeded normally from that point with all ADPs well-behaved and with the agreement factors improved by several %. All silyl groups had one or alkyl groups further disordered over two positions; these were located with some difficulty because the difference maps were always contaminated by density from another silyl group related by the twofold axis. Each independent Si(*i*-Pr)$_3$ group and each individual Si-C_3H_7 moiety was made similar with SAME instructions.

Due to the special-position disorder, a RIGU restraint was required for all atoms. Disordered silyl groups were further restrained with SIMU instructions. Hydrogen atoms were placed in calculated positions and refined with riding isotropic ADPs and coordinates.

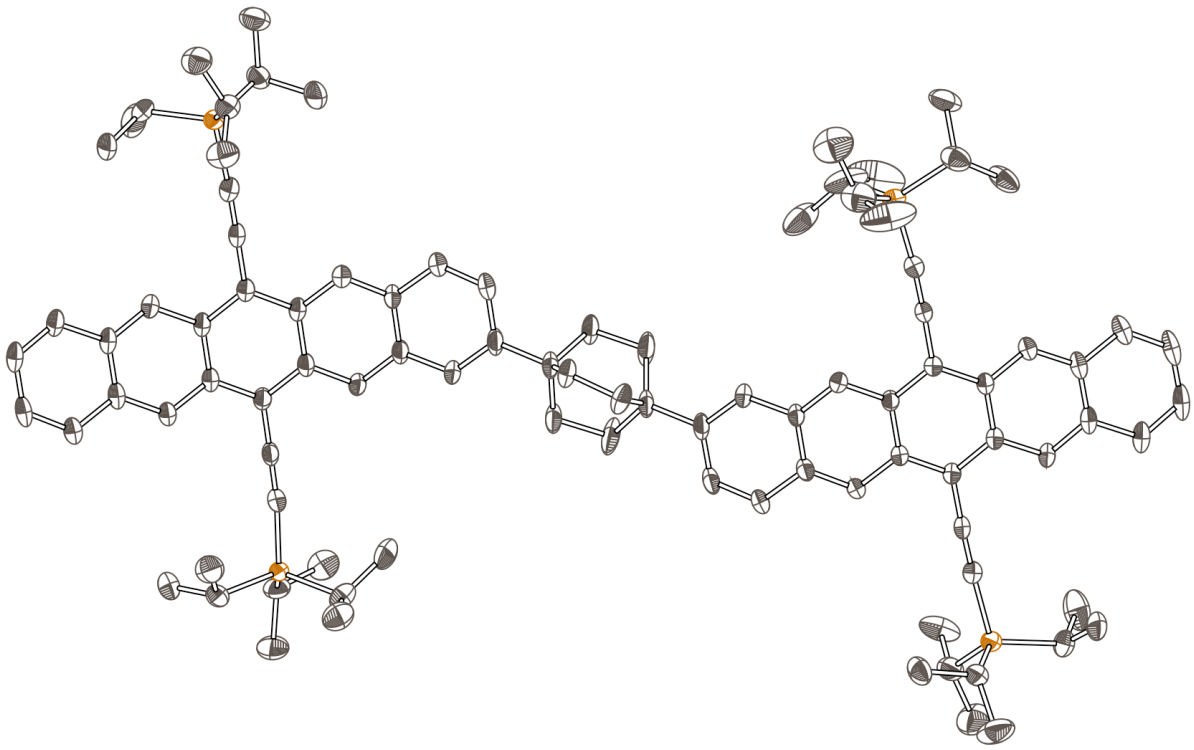

FIGURE S18: Molecular structure of **BCO**. Hydrogen atoms and the minor positions of disordered atoms are omitted for clarity.

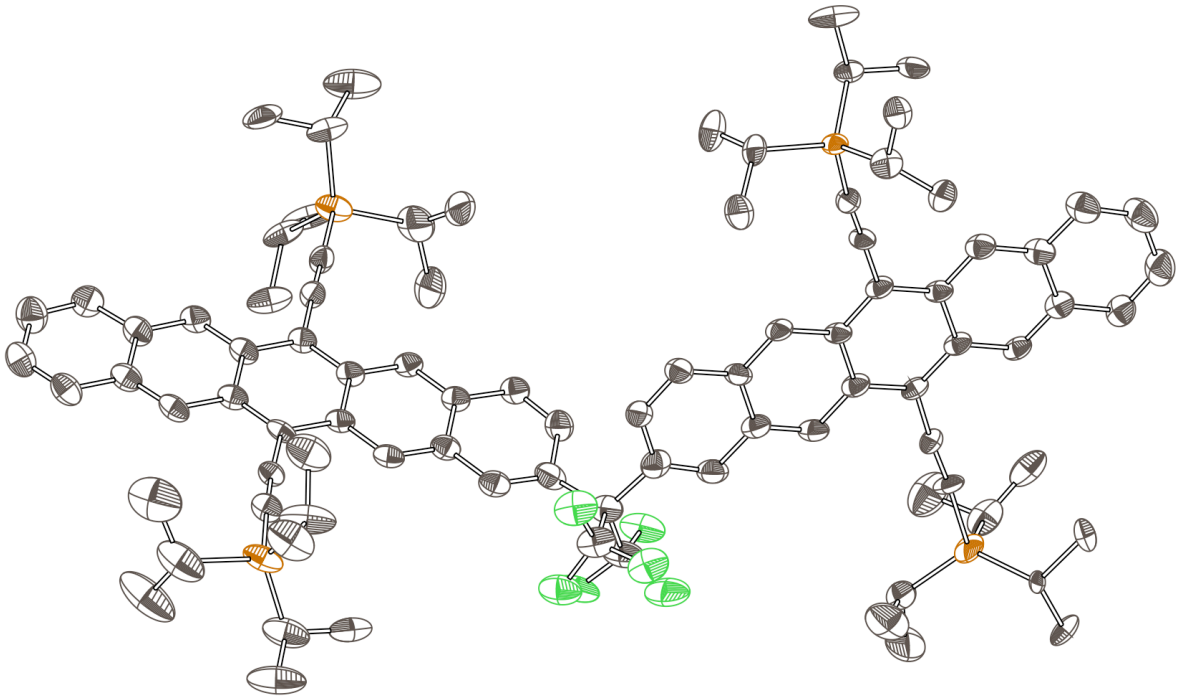

FIGURE S19: Molecular structure of **TFM**. Hydrogen atoms and the minor positions of disordered atoms are omitted for clarity.

Compound	BCO	TFM
Formula	$C_{96}H_{118}Si_4$	$C_{91}H_{106}F_6Si_4$
MW	1384.26	1426.11
Space group	P-1	C2/c
a **(Å)**	8.93370(19)	26.5637(5)
b **(Å)**	20.7978(5)	7.89746(9)
c **(Å)**	23.4696(6)	41.3109(9)
α **(°)**	98.332(2)	90
β **(°)**	90.9598(18)	106.605(2)
γ **(°)**	95.4335(19)	90
V (Å^3)	4293.21(17)	8305.0(3)
Z	2	4
ρ_{calc} (g cm^{-3})	1.071	1.141
T (K)	100	100
λ (Å)	1.54184	1.54184
$2\theta_{min}$, $2\theta_{max}$	9, 143	9, 143
Nref	77120	136992
R(int), R(σ)	.0741, .0564	.0544, .0167
μ(mm^{-1})	0.959	1.113
Size (mm)	.26 x .11 x .04	.25 x .18 x .03
T_{max}, T_{min}	.967, .871	.971, .801
Data	16580	8069
Restraints	1761	3210
Parameters	1346	1148
R_1(obs)	0.0931	0.0726
wR_2(all)	0.2655	0.2035
S	1.074	1.107
Peak, hole (e$^-$ Å^{-3})	0.76, -0.39	0.41, -0.30

4. GENERAL METHODS

All commercially obtained reagents/solvents were used as received; chemicals were purchased from Alfa Aesar®, Sigma-Aldrich®, Acros organics®, TCI America®, Mallinckrodt®, and Oakwood® Products, and were used as received without further purification. Unless stated otherwise, reactions were conducted in oven-dried glassware under argon atmosphere. The yields reported in the synthesis are not optimized. ^{1}H-NMR and ^{13}C-NMR spectra were recorded on Bruker 400 MHz (100 MHz for ^{13}C) and on 500 MHz (125 MHz for ^{13}C) spectrometers. Data from the ^{1}H-NMR and ^{13}C spectroscopy are reported as chemical shift (δ ppm) with the corresponding integration values. Coupling constants (*J*) are reported in hertz (Hz). Standard abbreviations indicating multiplicity were used as follows: s (singlet), b (broad), d (doublet), t (triplet), q (quartet), m (multiplet) and virt (virtual). The mass spectral data for the compounds were obtained from XEVO G2-XS Waters® equipped with a QTOF detector with multiple inlet and ionization capabilities including electrospray ionization (ESI), atmospheric pressure chemical ionization (APCI), and atmospheric solids analysis probe (ASAP). The base peaks were usually obtained as $[M]^{+}$ or $[M+H]^{+}$ ions.

Anhydrous solvents were obtained from a Schlenk manifold with purification columns packed with activated alumina and supported copper catalyst (Glass Contour, Irvine, CA). All reactions were carried out under argon unless otherwise noted.

Electron Spin Resonance Studies:

Pulsed laser, continuous microwave and pulsed laser, pulsed microwave measurements were carried out using the method described in our previous report.[16] **BCO** and **Spiro** were dissolved in toluene and transferred to a sealed quartz ESR tube under a nitrogen environment. UV-visible absorption spectroscopy was used to ensure that no aggregation had occurred. Experiments were undertaken using a Bruker Elexsys E580. he samples were transferred to a cryogenically cooled (Oxford Instruments, CF935) resonator (Bruker, MD5) attached to an X-band microwave source (Bruker, Super X FT-ESR Bridge). A ~7 ns 599 nm laser pulse was used to excite the sample (Opotek, OPOLETTE). In **BCO** nutation frequency measurements, the nutation pulse was applied 1.7 μs and 700 ns after the laser pulse at 362.6 mT (9.626926 GHz) and 349.4 mT (9.626885 GHz), respectively. The data was Fourier transformed to establish the nutation frequency of a given transition.

4.1. General protocol for the synthesis of bridge derivatives

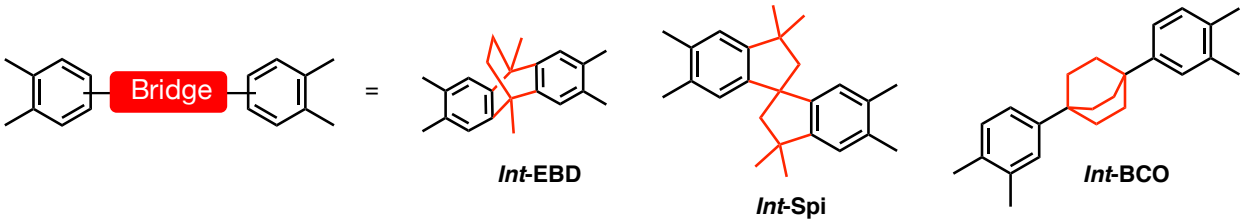

4.2. General protocol for the synthesis of bridge derivatives

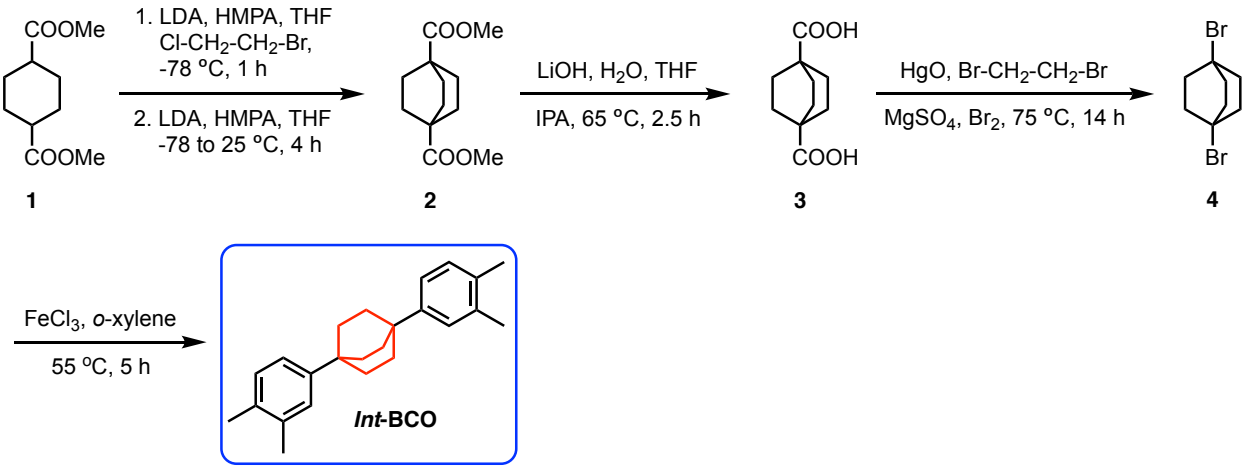

The compounds ***Int*-EBD**[17], ***Int*-Spi**[18] and **4**[19-21] were synthesized using procedures reported in the literature.

4.3. Synthesis of Pentacene Dimers with Homo/Nonconjugated bridge:

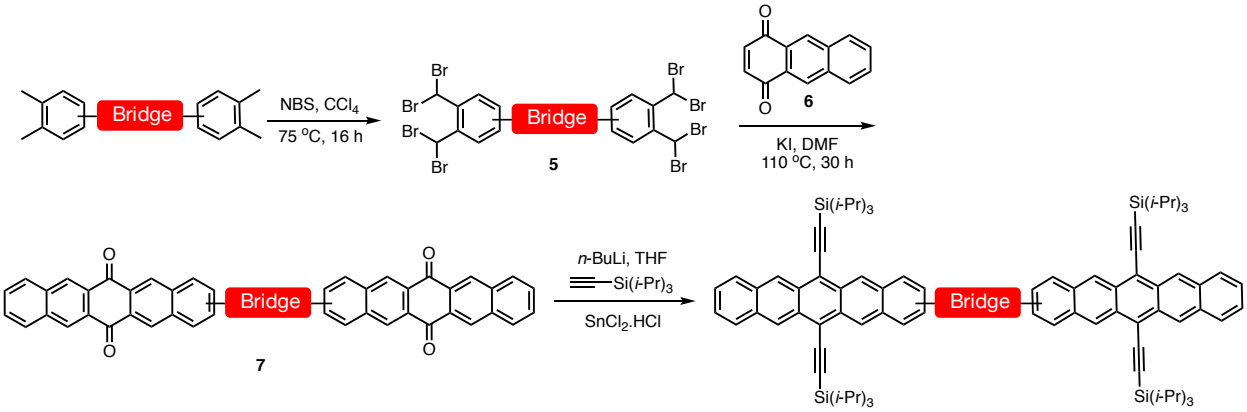

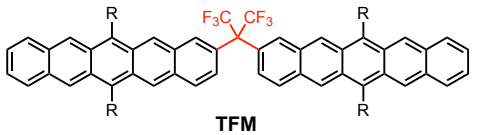

TFM

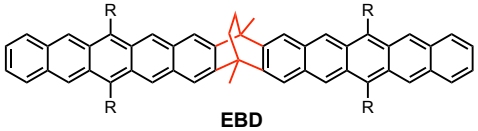

EBD

R = Si(*i*-Pr)$_3$

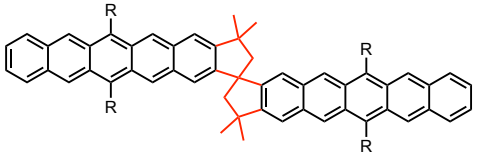

Spi

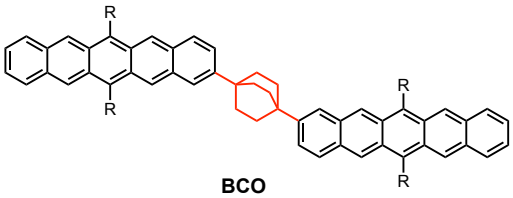

BCO

4.4. Synthesis of 1,4-bis(3,4-dimethylphenyl)bicyclo[2.2.2]octane:

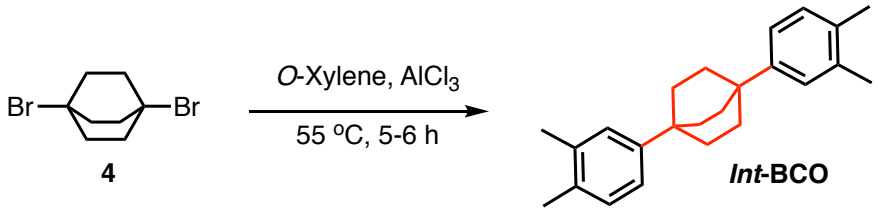

The compound **SP-3** was synthesized according to a procedure reported in the literature. To a solution of 1,4-dibromobicyclo[2.2.2]octane **4**[19-21] in dry *o*-xylene under argon atmosphere added *anhyd.* $AlCl_3$ and the mixture was stirred at room temperature for 10 minutes. The mixture heated to 55 °C and maintained for 5-6 h. The reaction was monitored by NMR spectroscopy and after the reaction was complete the solution was cooled to room temperature. The solution was quenched with cold water and the aqueous layer was extracted with ethyl acetate. The combined organic layer was washed with water and brine solution. The organic layer was dried over *anhyd.* Na_2SO_4, filter and concentrated to get the crude. The crude was purified by column chromatography using hexanes:ethyl acetate mixture to get the pure product.

Yield: 70% pale white solid

^{1}H-NMR (400 MHz, $CDCl_3$, δ ppm): 7.21 (s, 2H), 7.18-7.13 (m, 4H), 2.33 (s, 6H), 2.29 (s, 3H) and 2.00 (s, 12H).

^{13}C-NMR (100 MHz, $CDCl_3$, δ ppm): 147.6, 136.1, 133.7, 129.4, 126.97, 122.9, 34.6, 32.95, 20.1 and 19.3.

MS (ASAP): Calculated $[M]^+$: 318.2348; Observed: 318.2347.

4.5. Synthesis of Octabromo Derivatives:

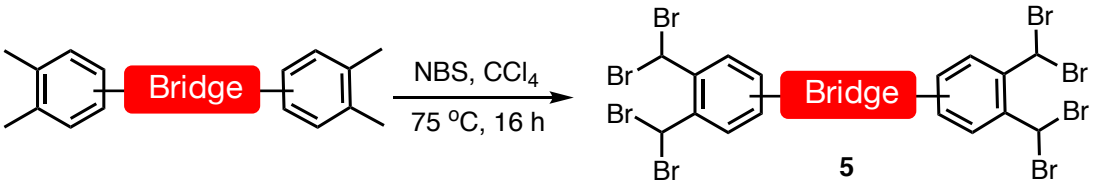

To a mixture of tetramethyl derivative 0.5 g in CCl_4 (15 mL) at room temperature under N_2 atmosphere added benzoyl peroxide and N-bromosuccinimide (4.2 *equiv.).* The mixture was heated to 80 ^oC and maintained for 4 h. The second portion of benzoyl peroxide and N-bromosuccinimide (4.2 *equiv.)* was added and the reaction was continued for further 12 h. The reaction was cooled and filtered off succinimide. The solid was washed with minimal amount of DCM. The combined organic layer was washed with 1N NaOH (15 mL), DM water (15 mL) and brine solution (15 mL). The organic layer was dried, filtered and concentrated to get the crude. The crude was directly taken to next step.

Note: Complete octabromination was not observed. Nevertheless, the material obtained was taken to next step.

4.6. Synthesis of Bipentacenequinone Derivative:

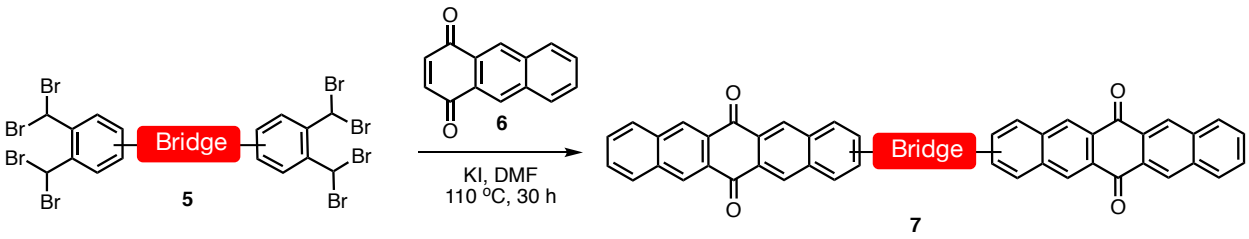

A mixture of octabromo derivative 1.6 g, KI (12 *equiv.*) and the quinone (2.2 *equiv.*) in dry DMF (30 mL) under argon atmosphere was heated to 110 °C and maintained for 30 h. After the reaction, the mixture was cooled to room temperature and diluted DM water (30 mL) stirred for 10 minutes and filtered. The solid was washed with methanol and acetone. The solid was directly taken to next step without further purification.

4.7. Synthesis of Homo/Nonconjugated Bipentacene:

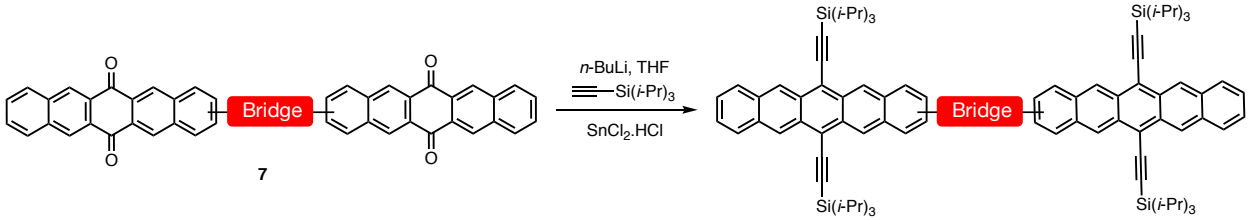

7

To a solution of (triisopropylsilyl)acetylene (12 equiv.) in dry and degassed THF (25 mL) in 250 mL two neck flask at 0 °C added *n*-butyl lithium (11.5 equiv., 2.5 M in hexanes). This solution was allowed to stir at 30 minutes followed by the addition of pentacenequinone (0.6 g, 1.0 equiv.) under positive argon flow. The solution was allowed to warm to room temperature and stirred overnight during which the solid pentacenequinone was completely dissolved. To this clear, deep yellow solution was added of a saturated solution of tin (II) chloride dihydrate (10 equiv.) in 10% aqueous HCl solution (8 mL) during which the solution turned deep blue. The resulting mixture was stirred at rt for 1 h under dark and filtered over a pad of silica. The solid was washed with DCM and the combined organic layer was washed with water (2 × 20 mL), dried over *anhyd.* Na_2SO_4, filtered and the solvent was removed under reduced pressure to get the crude product. The crude was purified by silica chromatography using mixture of DCM:hexanes as an eluent to obtain pentacene dimer derivatives.

Yield = 17% (for three steps); MS (ES+): Calculated $[M]^+$: 1354.7998; Observed: 1354.8072.
^{1}H-NMR (500 MHz, $CDCl_3$, δ ppm): 9.31 (s, 4H), 9.28 (s, 4H), 7.99-7.97 (m, 4H), 7.85 (s, 4H), 7.43-7.41 (m, 4H), 2.28 (s, 6H), 2.01 (s, 4H) and 1.48-1.40 (m, 84H).

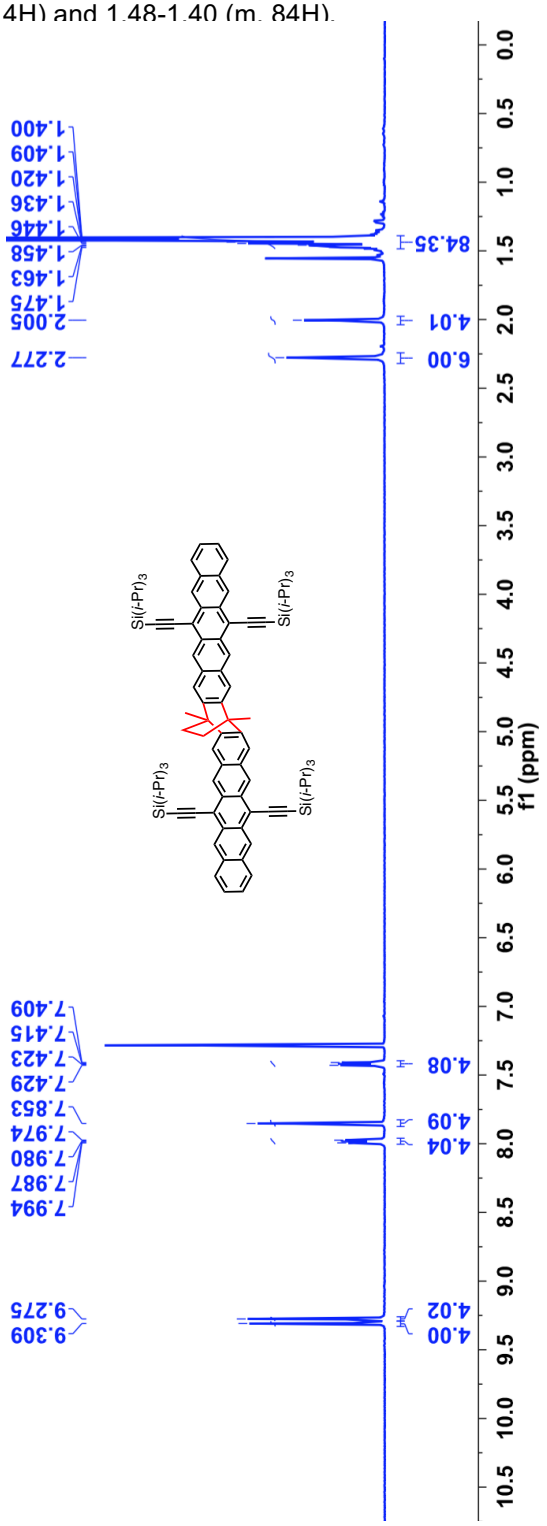

^{13}C-NMR (125 MHz, $CDCl_3$, δ ppm): 144.3, 132.1, 131.8, 130.7, 130.5, 128.7, 126.2, 125.9, 125.7, 119.1, 118.0, 106.8, 104.9, 41.2, 35.2, 19.1, 18.95 and 11.7.

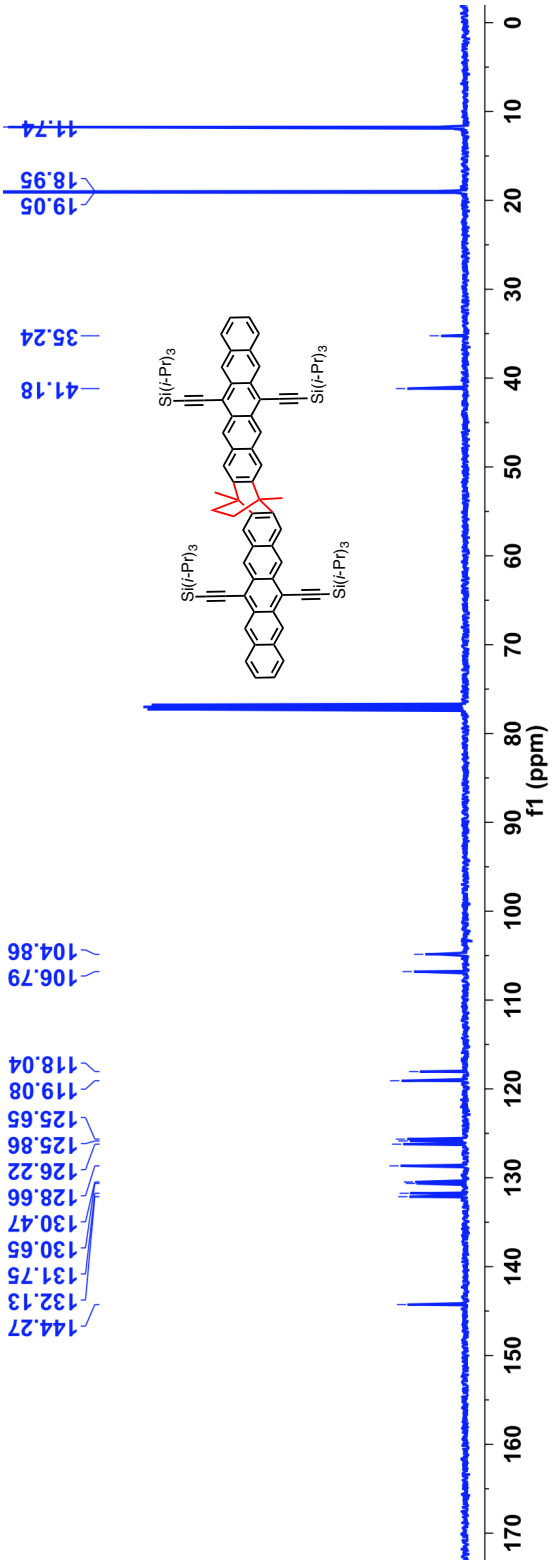

Yield = 15% (for three steps); MS (ES+): Calculated $[M]^+$: 1396.8467; Observed: 1396.8496.
^{1}H-NMR (400 MHz, $CDCl_3$, δ ppm): 9.35 (s, 2H), 9.33 (s, 2H), 9.28 (s, 2H), 9.14 (s, 2H), 7.99-7.94 (m, 4H), 7.83 (s, 2H), 7.51 (s, 2H), 7.42-7.39 (m, 4H), 2.71-2.62 (m, 4H), 1.73 (s, 6H), 1.63 (s, 6H), 1.48-1.43 (m, 42H) and 1.24-1.21 (m, 42H).

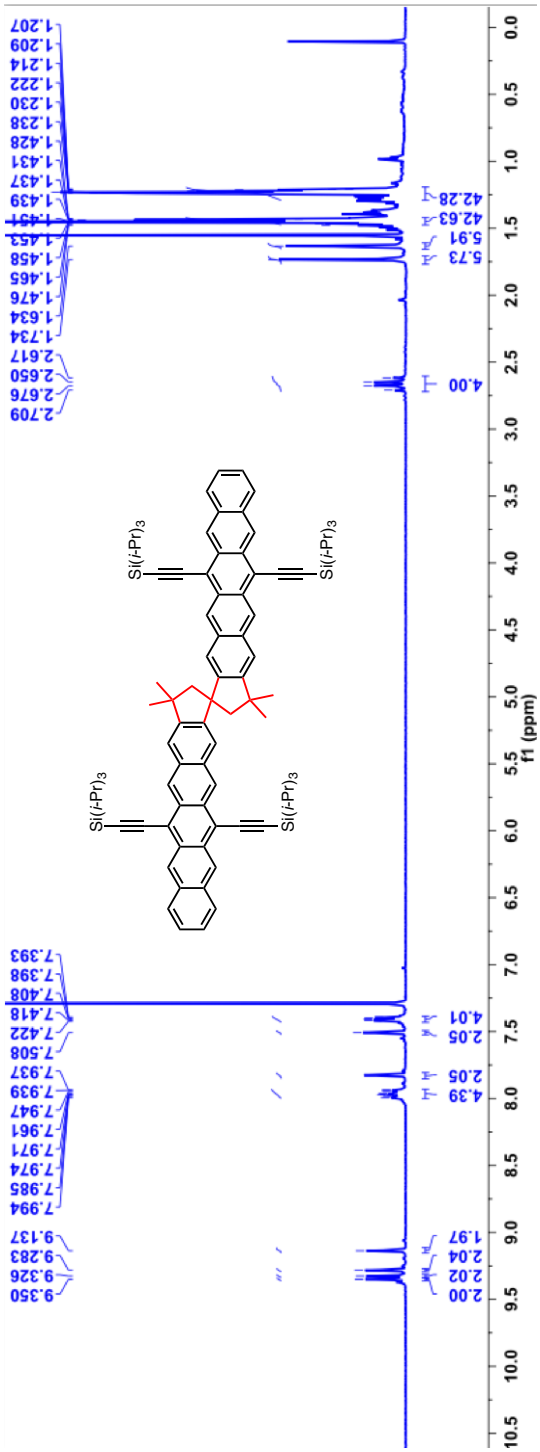

^{13}C-NMR (125 MHz, $CDCl_3$, δ ppm): 153.2, 152.96, 132.9, 132.8, 132.2, 130.7, 130.5, 130.3, 128.7, 126.3, 126.2, 125.9, 125.4, 123.1, 120.1, 118.2, 117.9, 107.2, 106.8, 104.99, 104.7, 60.3, 56.9, 43.2, 32.0, 30.7, 19.1, 18.9, 11.8 and 11.6.

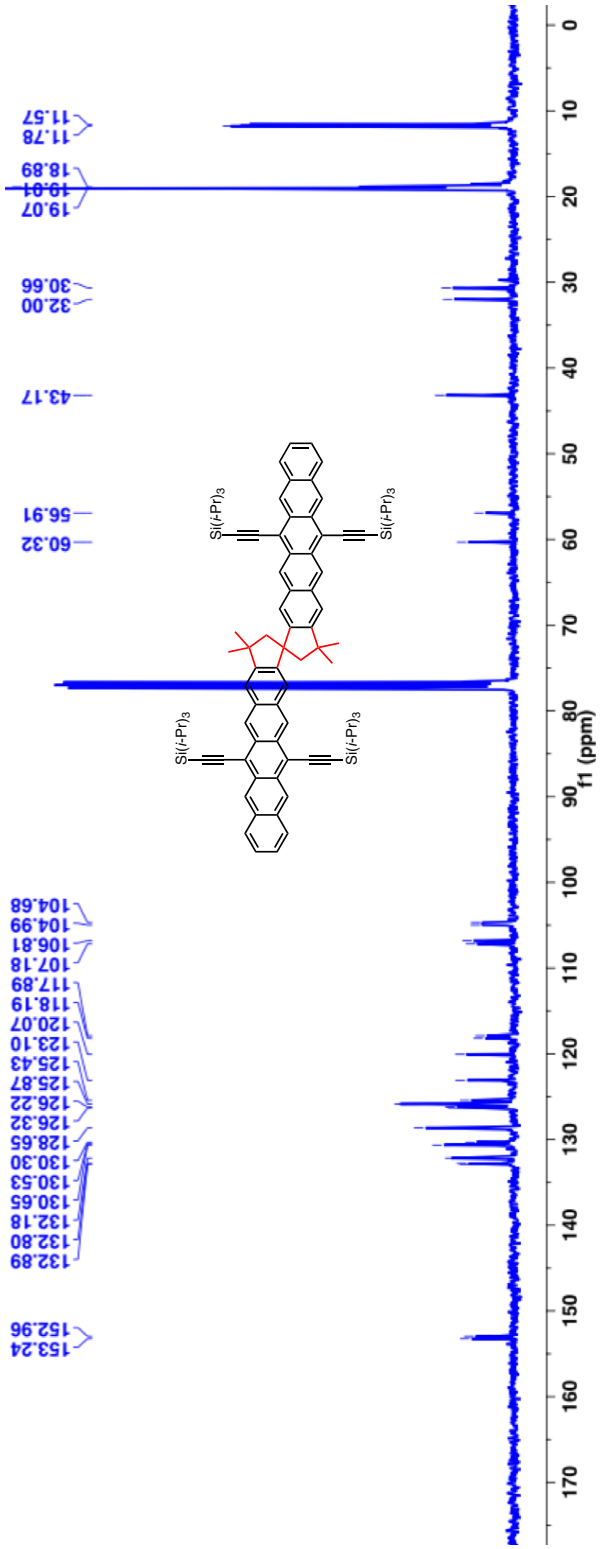

^{1}H-NMR (400 MHz, $CDCl_3$, δ ppm): 7.21 (s, 2H), 7.18-7.13 (m, 4H), 2.33 (s, 6H), 2.29 (s, 3H) and 2.00 (s, 12H).

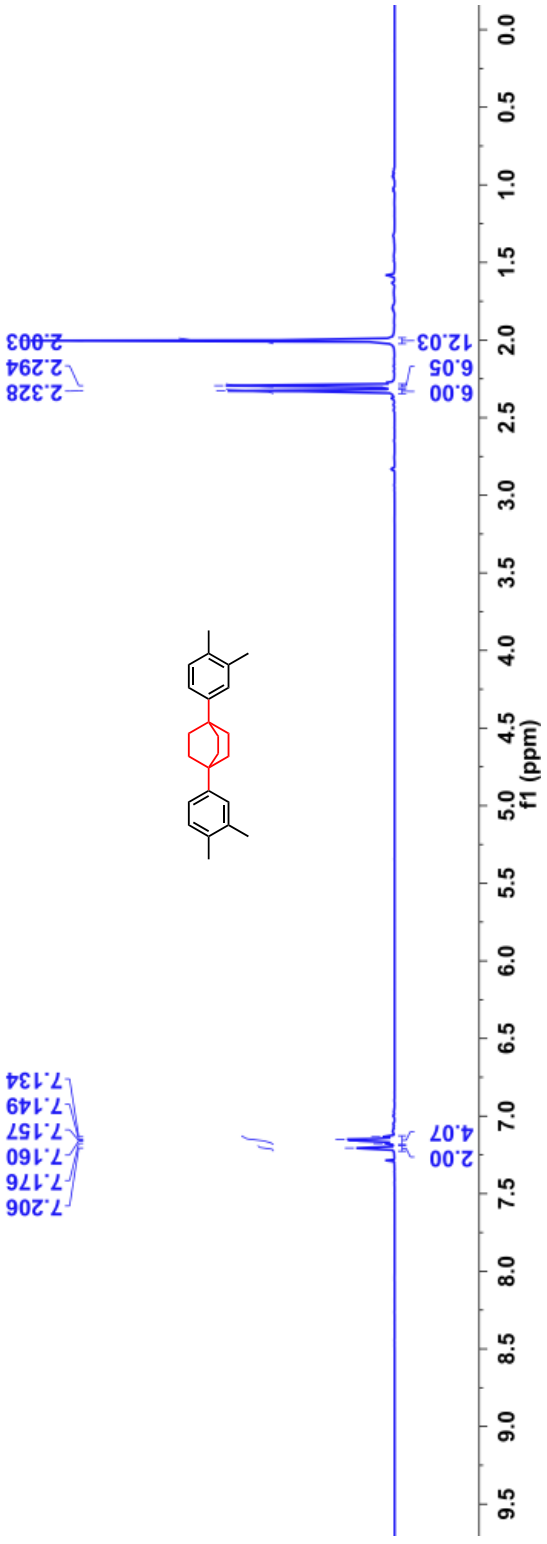

^{13}C-NMR (125 MHz, $CDCl_3$, δ ppm): 147.6, 136.1, 133.7, 129.4, 126.97, 122.9, 34.6, 32.95, 20.1 and 19.3.

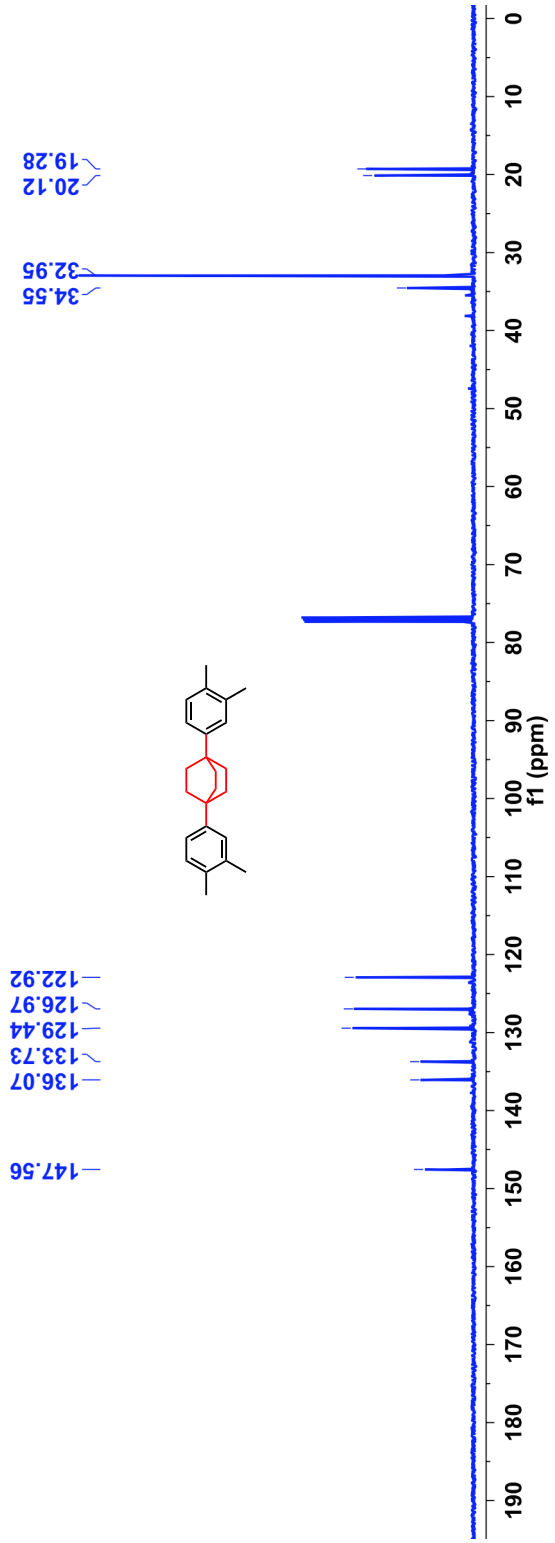

Yield = 19% (for three steps); MS (ES+): Calculated $[M]^+$: 1382.8311; Observed: 1382.8315.

^{1}H-NMR (500 MHz, $CDCl_3$, δ ppm): 9.34-9.29 (m, 8H), 8.01-7.98 (s, 6H), 7.85 (s, 2H), 7.62-7.59 (m, 2H), 7.45-7.43 (m, 4H), 2.24 (s, 12H) and 1.43-1.39 (m, 84H).

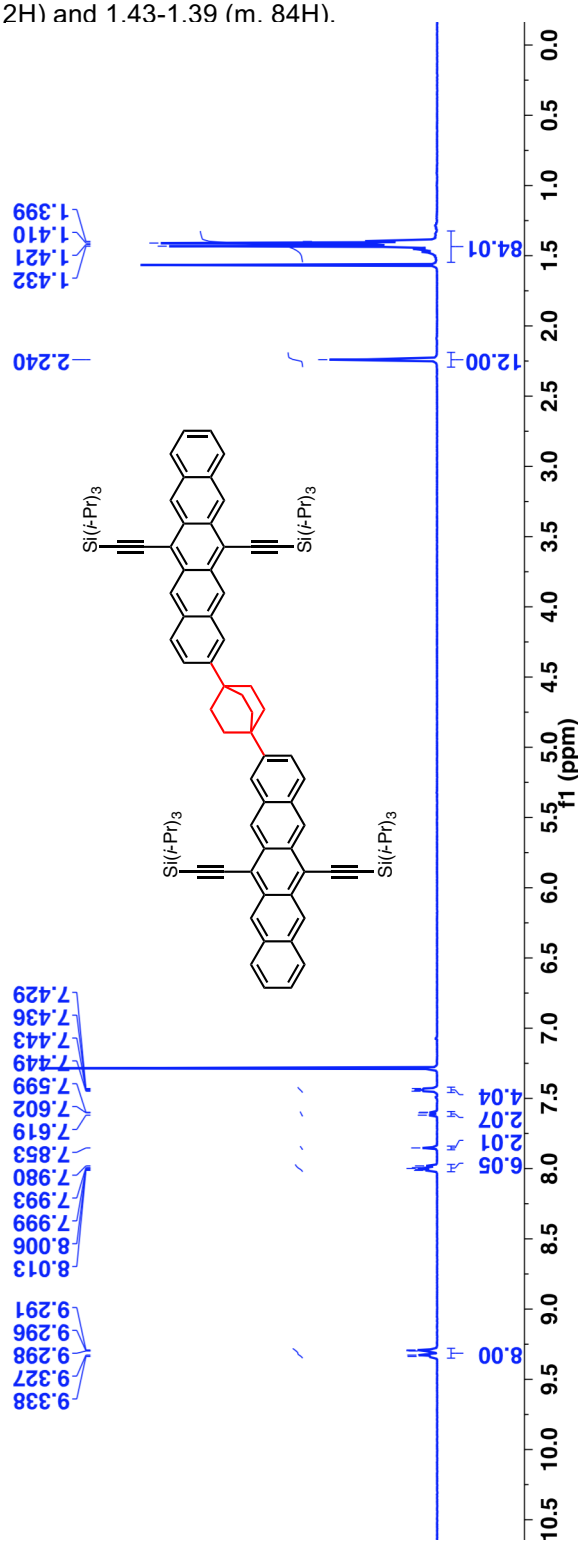

^{13}C-NMR (125 MHz, $CDCl_3$, δ ppm): 147.1, 132.5, 132.3, 132.2, 131.3, 130.9, 130.6, 130.5, 128.7, 128.4, 126.3, 125.97, 125.9, 125.7, 123.0, 118.3, 118.1, 106.97,104.8, 35.6, 31.97, 19.1, 19.0, 11.74 and 11.72.

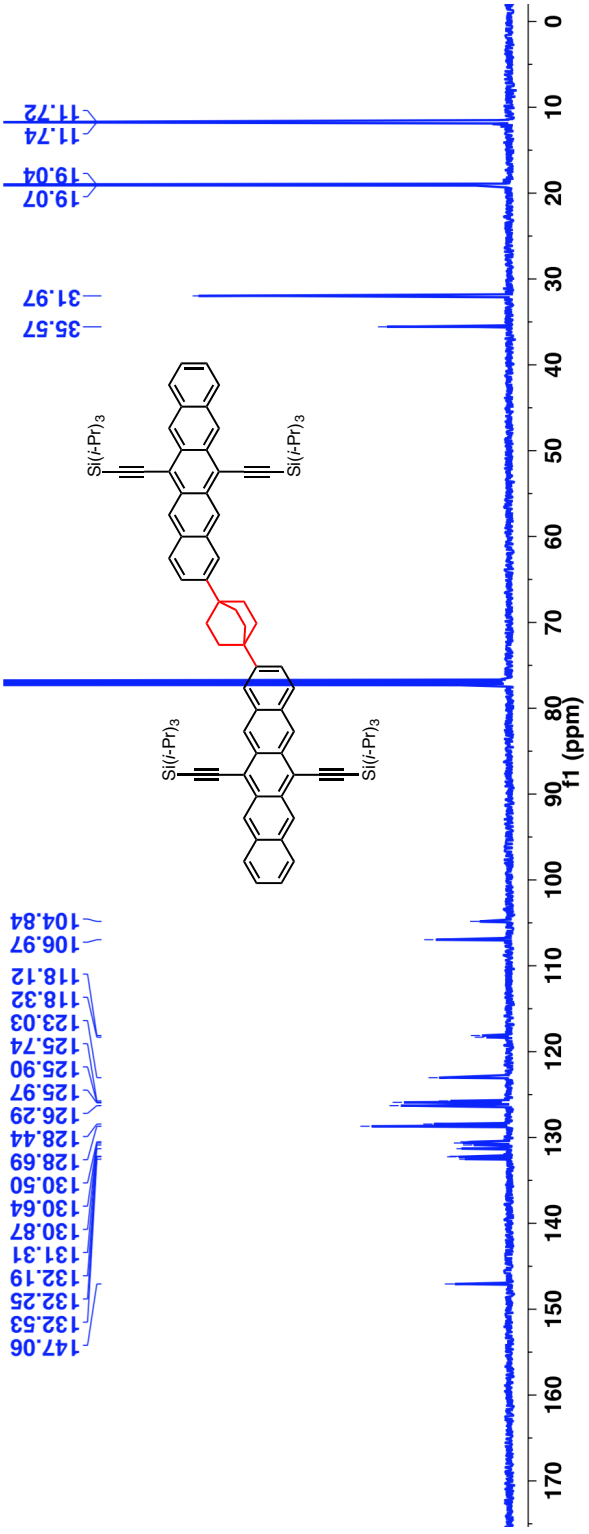

5. REFERENCES

(1) Sanders, S. N.; Kumarasamy, E.; Pun, A. B.; Trinh, M. T.; Choi, B.; Xia, J.; Taffet, E. J.; Low, J. Z.; Miller, J. R.; Roy, X.; Zhu, X. Y.; Steigerwald, M. L.; Sfeir, M. Y.; Campos, L. M. *J. Am. Chem. Soc.* **2015**, *137*, 8965.

(2) Scholes, G. D. *J. Phys. Chem. A* **2015**, *119*, 12669.

(3) Snellenburg, J. J. L., S. P.; Seger, R.; Mullen, K. M.; van Stokum, I. H. M. *J. Stat. Soft.* **2012**, *49*, 1.

(4) Snyder, L. R.; Kirkland, J. J.; Glajch, J. L. In *Practical HPLC Method Development*; John Wiley & Sons, Inc.: 1997, p 721.

(5) Bosque, R.; Sales, J. *J. Chem. Inform. Comput. Sci.* **2002**, *42*, 1154.

(6) Fuemmeler, E. G.; Sanders, S. N.; Pun, A. B.; Kumarasamy, E.; Zeng, T.; Miyata, K.; Steigerwald, M. L.; Zhu, X. Y.; Sfeir, M. Y.; Campos, L. M.; Ananth, N. *ACS Cent. Sci.* **2016**, *2*, 316.

(7) Schmidt, M. W.; Baldridge, K. K.; Boatz, J. A.; Elbert, S. T.; Gordon, M. S.; Jensen, J. H.; Koseki, S.; Matsunaga, N.; Nguyen, K. A.; Su, S.; Windus, T. L.; Dupuis, M.; Montgomery, J. A. *J. Comput. Chem.* **1993**, *14*, 1347.

(8) Towns, J.; Cockerill, T.; Dahan, M.; Foster, I.; Gaither, K.; Grimshaw, A.; Hazlewood, V.; Lathrop, S.; Lifka, D.; Peterson, G. D. *Comput. Sci. Eng.* **2014**, *16*, 62.

(9) Zeng, T.; Hoffmann, R.; Ananth, N. *J. Am. Chem. Soc.* **2014**, *136*, 5755.

(10) Feng, X.; Luzanov, A. V.; Krylov, A. I. *J. Phys. Chem. Lett.* **2013**, *4*, 3845.

(11) Pieniazek, P. A. K., A. I.; Bradforth, S. E. *J. Chem. Phys.* **2007**, *127*, 044317.

(12) Blanc, E.; Schwarzenbach, D.; Flack, H. D. *J. Appl. Crystallogr.* **1991**, *24*, 1035.

(13) Clark, R. C.; Reid, J. S. *Act. Cryst. A* **1995**, *51*, 887.

(14) Sheldrick, G. M. *Act. Cryst. A* **2008**, *64*, 112.

(15) Dolomanov, O. V.; Bourhis, L. J.; Gildea, R. J.; Howard, J. A. K.; Puschmann, H. *J. Appl. Crystallogr.* **2009**, *42*, 339.

(16) Tayebjee, M. J. Y.; Sanders, S. N.; Kumarasamy, E.; Campos, L. M.; Sfeir, M. Y.; McCamey, D. R. *Nat. Phys.* **2017**, *13*, 182.

(17) Rogan, Y.; Malpass-Evans, R.; Carta, M.; Lee, M.; Jansen, J. C.; Bernardo, P.; Clarizia, G.; Tocci, E.; Friess, K.; Lanc, M.; McKeown, N. B. *J. Mater. Chem. A* **2014**, *2*, 4874.

(18) Rogan, Y.; Starannikova, L.; Ryzhikh, V.; Yampolskii, Y.; Bernardo, P.; Bazzarelli, F.; Jansen, J. C.; McKeown, N. B. *Polym. Chem.* **2013**, *4*, 3813.

(19) Royalty, S. M.; Burns, J. F.; Scicinski, J. J.; Jagdmann, J. G. E.; Foglesong, R. J.; Griffin, K. R.; Dyakonov, T.; Middlemiss, D. WO 2006012395 A2; **2006**.

(20) Bennett, B. L.; Elsner, J.; Erdman, P.; Hilgraf, R.; LeBrun, L. A.; McCarrick, M.; Moghaddam, M. F.; Nagy, M. A.; Norris, S.; Paisner, D. A. US2013/0029987A1, **2013**.

(21) Wiberg, K. B.; Pratt, W. E.; Bailey, W. F. *J. Am. Chem. Soc.* **1977**, *99*, 2297.

Coordinates used for calculations

Given in GAMESS output notation (Angstroms)

EBD

ATOM	CHARGE	X	Y	Z
C	6.0	5.5180424259	-0.7258637658	-0.1341005503
C	6.0	-5.5180424259	-0.7258637658	-0.1341005503
C	6.0	5.5180424259	0.7258637658	-0.1341005503
C	6.0	-5.5180424259	0.7258637658	-0.1341005503
C	6.0	3.3602458282	-0.7243811707	-1.3012709245
C	6.0	-3.3602458282	-0.7243811707	-1.3012709245
C	6.0	3.3602458282	0.7243811707	-1.3012709245
C	6.0	-3.3602458282	0.7243811707	-1.3012709245
C	6.0	6.6066446899	1.4299139543	0.4506827555
C	6.0	-6.6066446899	1.4299139543	0.4506827555
C	6.0	6.6066446899	-1.4299139543	0.4506827555
C	6.0	-6.6066446899	-1.4299139543	0.4506827555
C	6.0	4.4261449419	1.4025487660	-0.7232958950
C	6.0	-4.4261449419	1.4025487660	-0.7232958950
C	6.0	4.4261449419	-1.4025487660	-0.7232958950
C	6.0	-4.4261449419	-1.4025487660	-0.7232958950
H	1.0	4.4279308162	2.4883591662	-0.7219974607
H	1.0	-4.4279308162	2.4883591662	-0.7219974607
H	1.0	4.4279308162	-2.4883591662	-0.7219974607
H	1.0	-4.4279308162	-2.4883591662	-0.7219974607
C	6.0	1.2193385847	0.7241208054	-2.4704735589
C	6.0	-1.2193385847	0.7241208054	-2.4704735589
C	6.0	1.2193385847	-0.7241208054	-2.4704735589

C	6.0	-1.2193385847	-0.7241208054	-2.4704735589
C	6.0	9.8621094279	-0.7249790365	2.1897199296
C	6.0	-9.8621094279	-0.7249790365	2.1897199296
C	6.0	9.8621094279	0.7249790365	2.1897199296
C	6.0	-9.8621094279	0.7249790365	2.1897199296
C	6.0	7.6977556434	-0.7258102327	1.0347208066
C	6.0	-7.6977556434	-0.7258102327	1.0347208066
C	6.0	7.6977556434	0.7258102327	1.0347208066
C	6.0	-7.6977556434	0.7258102327	1.0347208066
C	6.0	8.7904982308	1.4029204233	1.6183603603
C	6.0	-8.7904982308	1.4029204233	1.6183603603
C	6.0	8.7904982308	-1.4029204233	1.6183603603
C	6.0	-8.7904982308	-1.4029204233	1.6183603603
H	1.0	8.7882815382	2.4887174658	1.6175157518
H	1.0	-8.7882815382	2.4887174658	1.6175157518
H	1.0	8.7882815382	-2.4887174658	1.6175157518
H	1.0	-8.7882815382	-2.4887174658	1.6175157518
C	6.0	6.6066304186	2.8539057227	0.4512008934
C	6.0	-6.6066304186	2.8539057227	0.4512008934
C	6.0	6.6066304186	-2.8539057227	0.4512008934
C	6.0	-6.6066304186	-2.8539057227	0.4512008934
C	6.0	2.2536668311	1.4124696488	-1.9049975337
C	6.0	-2.2536668311	1.4124696488	-1.9049975337
C	6.0	2.2536668311	-1.4124696488	-1.9049975337
C	6.0	-2.2536668311	-1.4124696488	-1.9049975337
H	1.0	2.2671986721	2.4988387170	-1.8973389611
H	1.0	-2.2671986721	2.4988387170	-1.8973389611
H	1.0	2.2671986721	-2.4988387170	-1.8973389611
H	1.0	-2.2671986721	-2.4988387170	-1.8973389611

C	6.0	6.6070521805	-4.0664745352	0.4523763367
C	6.0	-6.6070521805	-4.0664745352	0.4523763367
C	6.0	6.6070521805	4.0664745352	0.4523763367
C	6.0	-6.6070521805	4.0664745352	0.4523763367
C	6.0	10.9746431895	-1.4110297395	2.7817114837
C	6.0	-10.9746431895	-1.4110297395	2.7817114837
C	6.0	10.9746431895	1.4110297395	2.7817114837
C	6.0	-10.9746431895	1.4110297395	2.7817114837
H	1.0	10.9714811913	-2.4986052053	2.7802860351
H	1.0	-10.9714811913	-2.4986052053	2.7802860351
H	1.0	10.9714811913	2.4986052053	2.7802860351
H	1.0	-10.9714811913	2.4986052053	2.7802860351
C	6.0	12.0140258883	-0.7161056799	3.3340929345
C	6.0	-12.0140258883	-0.7161056799	3.3340929345
C	6.0	12.0140258883	0.7161056799	3.3340929345
C	6.0	-12.0140258883	0.7161056799	3.3340929345
H	1.0	12.8516575688	-1.2469393011	3.7793351368
H	1.0	-12.8516575688	-1.2469393011	3.7793351368
H	1.0	12.8516575688	1.2469393011	3.7793351368
H	1.0	-12.8516575688	1.2469393011	3.7793351368
C	6.0	0.0000000000	1.3385107451	-3.1576804543
C	6.0	0.0000000000	-1.3385107451	-3.1576804543
C	6.0	0.0000000000	2.8659045974	-3.1761074974
C	6.0	0.0000000000	-2.8659045974	-3.1761074974
C	6.0	0.0000000000	0.7753214326	-4.6198725047
C	6.0	0.0000000000	-0.7753214326	-4.6198725047
H	1.0	0.0000000000	3.2846196066	-2.1636616091
H	1.0	0.0000000000	-3.2846196066	-2.1636616091
H	1.0	0.8842969123	3.2451113968	-3.6999135835

H	1.0	-0.8842969123	3.2451113968	-3.6999135835
H	1.0	0.8842969123	-3.2451113968	-3.6999135835
H	1.0	-0.8842969123	-3.2451113968	-3.6999135835
H	1.0	-0.8821775125	1.1648646590	-5.1410520023
H	1.0	0.8821775125	1.1648646590	-5.1410520023
H	1.0	-0.8821775125	-1.1648646590	-5.1410520023
H	1.0	0.8821775125	-1.1648646590	-5.1410520023
H	1.0	6.6077334965	-5.1330825695	0.4534940786
H	1.0	-6.6077334965	-5.1330825695	0.4534940786
H	1.0	6.6077334965	5.1330825695	0.4534940786
H	1.0	-6.6077334965	5.1330825695	0.4534940786

TFM

ATOM	CHARGE	X	Y	Z
C	6.0	0.0000000000	0.0000000000	-2.4754392942
C	6.0	0.2424041412	-1.2332836133	-3.3989145896
C	6.0	-0.2424041412	1.2332836133	-3.3989145896
F	9.0	1.2001219835	-1.0087309991	-4.3255429487
F	9.0	-1.2001219835	1.0087309991	-4.3255429487
F	9.0	0.6283879784	-2.3119978423	-2.6853090683
F	9.0	-0.6283879784	2.3119978423	-2.6853090683
F	9.0	-0.8766879195	-1.5745405831	-4.0588379615
F	9.0	0.8766879195	1.5745405831	-4.0588379615
C	6.0	-1.2129618171	-0.3317585977	-1.5768363646
C	6.0	1.2129618171	0.3317585977	-1.5768363646
C	6.0	-2.4665282229	0.1948297857	-1.7449606390
C	6.0	2.4665282229	-0.1948297857	-1.7449606390
H	1.0	-2.6914991438	0.8775068569	-2.5553220531

H	1.0	2.6914991438	-0.8775068569	-2.5553220531
C	6.0	-3.5359243020	-0.1169408633	-0.8391317348
C	6.0	3.5359243020	0.1169408633	-0.8391317348
C	6.0	-4.8015697609	0.4403700224	-0.9815139401
C	6.0	4.8015697609	-0.4403700224	-0.9815139401
H	1.0	-4.9949407381	1.1258767529	-1.8008346719
H	1.0	4.9949407381	-1.1258767529	-1.8008346719
C	6.0	-5.8564045922	0.1412642589	-0.0898583400
C	6.0	5.8564045922	-0.1412642589	-0.0898583400
C	6.0	-7.1517916234	0.7075120037	-0.2497225834
C	6.0	7.1517916234	-0.7075120037	-0.2497225834
C	6.0	-8.2081082056	0.3635826742	0.6401561525
C	6.0	8.2081082056	-0.3635826742	0.6401561525
C	6.0	-9.5125400878	0.8783906899	0.4776890824
C	6.0	9.5125400878	-0.8783906899	0.4776890824
H	1.0	-9.7032377808	1.5600415632	-0.3456055206
H	1.0	9.7032377808	-1.5600415632	-0.3456055206
C	6.0	-10.5566227273	0.5286726479	1.3272089796
C	6.0	10.5566227273	-0.5286726479	1.3272089796
C	6.0	-11.8890142532	1.0292278129	1.1481974886
C	6.0	11.8890142532	-1.0292278129	1.1481974886
H	1.0	-12.0793396466	1.7085803949	0.3206188652
H	1.0	12.0793396466	-1.7085803949	0.3206188652
C	6.0	-12.8970505140	0.6575262780	1.9928784576
C	6.0	12.8970505140	-0.6575262780	1.9928784576
H	1.0	-13.9036909993	1.0391324998	1.8438438159
H	1.0	13.9036909993	-1.0391324998	1.8438438159
C	6.0	-12.6424974790	-0.2382743404	3.0814362016
C	6.0	12.6424974790	0.2382743404	3.0814362016

H	1.0	-13.4603656327	-0.5197876433	3.7394447947
H	1.0	13.4603656327	0.5197876433	3.7394447947
C	6.0	-11.3876387009	-0.7367660915	3.2922710452
C	6.0	11.3876387009	0.7367660915	3.2922710452
H	1.0	-11.1902482097	-1.4188186179	4.1159763485
H	1.0	11.1902482097	1.4188186179	4.1159763485
C	6.0	-10.2995480568	-0.3797463905	2.4281604660
C	6.0	10.2995480568	0.3797463905	2.4281604660
C	6.0	-9.0157119961	-0.8822874666	2.6065727461
C	6.0	9.0157119961	0.8822874666	2.6065727461
H	1.0	-8.8191395625	-1.5640145078	3.4283342524
H	1.0	8.8191395625	1.5640145078	3.4283342524
C	6.0	-7.9521797431	-0.5486488785	1.7405897011
C	6.0	7.9521797431	0.5486488785	1.7405897011
C	6.0	-6.6493808218	-1.0922451010	1.9170451335
C	6.0	6.6493808218	1.0922451010	1.9170451335
C	6.0	-5.6023231057	-0.7717946291	1.0098860671
C	6.0	5.6023231057	0.7717946291	1.0098860671
C	6.0	-4.3108785196	-1.3257468685	1.1454559225
C	6.0	4.3108785196	1.3257468685	1.1454559225
H	1.0	-4.1197262046	-2.0083214932	1.9675933932
H	1.0	4.1197262046	2.0083214932	1.9675933932
C	6.0	-3.2864488119	-1.0272894477	0.2572694295
C	6.0	3.2864488119	1.0272894477	0.2572694295
C	6.0	-1.9733721939	-1.5846396739	0.3823419023
C	6.0	1.9733721939	1.5846396739	0.3823419023
H	1.0	-1.7760123510	-2.2772240312	1.1968215757
H	1.0	1.7760123510	2.2772240312	1.1968215757
C	6.0	-0.9808920161	-1.2518806206	-0.4898418016

C	6.0	0.9808920161	1.2518806206	-0.4898418016
H	1.0	0.0082258534	-1.6760167063	-0.3643496578
H	1.0	-0.0082258534	1.6760167063	-0.3643496578
C	6.0	-7.3937003297	1.6230057111	-1.3130768078
C	6.0	7.3937003297	-1.6230057111	-1.3130768078
C	6.0	-7.5955920142	2.4084168535	-2.2143862232
C	6.0	7.5955920142	-2.4084168535	-2.2143862232
C	6.0	-6.3917338661	-1.9733890461	3.0055184218
C	6.0	6.3917338661	1.9733890461	3.0055184218
C	6.0	-6.1661731192	-2.7219196200	3.9322839276
C	6.0	6.1661731192	2.7219196200	3.9322839276
H	1.0	7.7711081319	-3.1009342551	-3.0066038404
H	1.0	-7.7711081319	3.1009342551	-3.0066038404
H	1.0	5.9674782418	3.3801549867	4.7478442226
H	1.0	-5.9674782418	-3.3801549867	4.7478442226

Spi

ATOM	CHARGE	X	Y	Z
C	6.0	0.0000000000	0.0000000000	3.8556658184
C	6.0	0.1151713184	3.6121811211	3.6404526897
C	6.0	-0.1151713184	-3.6121811211	3.6404526897
C	6.0	0.1921190157	-1.2995958508	4.7218738236
C	6.0	-0.1921190157	1.2995958508	4.7218738236
C	6.0	0.8303419552	2.3958740289	4.2685511114
C	6.0	-0.8303419552	-2.3958740289	4.2685511114
C	6.0	1.2228398506	0.3361711665	3.0003202868
C	6.0	-1.2228398506	-0.3361711665	3.0003202868
C	6.0	1.6848868833	2.8764551587	5.4614454654
C	6.0	-1.6848868833	-2.8764551587	5.4614454654
C	6.0	1.6862921631	1.6738799076	3.2357846852
C	6.0	-1.6862921631	-1.6738799076	3.2357846852
C	6.0	1.8619825626	-0.4755007045	2.1048050481
C	6.0	-1.8619825626	0.4755007045	2.1048050481
C	6.0	2.7783215692	2.1618534232	2.5729810973
C	6.0	-2.7783215692	-2.1618534232	2.5729810973
C	6.0	3.0198713086	-0.0116424331	1.3977101505
C	6.0	-3.0198713086	0.0116424331	1.3977101505
C	6.0	3.4896828871	1.3417318060	1.6351892382
C	6.0	-3.4896828871	-1.3417318060	1.6351892382
C	6.0	3.7115582524	-0.8213202413	0.5021169399
C	6.0	-3.7115582524	0.8213202413	0.5021169399
C	6.0	4.6161846123	1.7958259521	0.9563967619
C	6.0	-4.6161846123	-1.7958259521	0.9563967619
C	6.0	4.7255019369	-3.6807638421	-1.5028129925

C	6.0	-4.7255019369	3.6807638421	-1.5028129925
C	6.0	4.8621418253	-0.3747318600	-0.1829548380
C	6.0	-4.8621418253	0.3747318600	-0.1829548380
C	6.0	5.1151890878	-2.5487293294	-1.3094306357
C	6.0	-5.1151890878	2.5487293294	-1.3094306357
C	6.0	5.3287067659	0.9812010281	0.0492707291
C	6.0	-5.3287067659	-0.9812010281	0.0492707291
C	6.0	5.5720028359	-1.2193917150	-1.0821978782
C	6.0	-5.5720028359	1.2193917150	-1.0821978782
C	6.0	6.4864456367	1.4536595778	-0.6309631438
C	6.0	-6.4864456367	-1.4536595778	-0.6309631438
C	6.0	6.7356363677	-0.7501992032	-1.7539267596
C	6.0	-6.7356363677	0.7501992032	-1.7539267596
C	6.0	6.9400763757	2.7849404404	-0.4086626253
C	6.0	-6.9400763757	-2.7849404404	-0.4086626253
C	6.0	7.1984573984	0.6076952608	-1.5274822940
C	6.0	-7.1984573984	-0.6076952608	-1.5274822940
C	6.0	7.3266951498	3.9188604095	-0.2199536238
C	6.0	-7.3266951498	-3.9188604095	-0.2199536238
C	6.0	7.4622966565	-1.5746460258	-2.6409835569
C	6.0	-7.4622966565	1.5746460258	-2.6409835569
C	6.0	8.3539835408	1.0512424276	-2.2077344657
C	6.0	-8.3539835408	-1.0512424276	-2.2077344657
C	6.0	8.6019542068	-1.1282192218	-3.3009732945
C	6.0	-8.6019542068	1.1282192218	-3.3009732945
C	6.0	9.0619622121	0.2294920578	-3.0784188836
C	6.0	-9.0619622121	-0.2294920578	-3.0784188836
C	6.0	9.3448788377	-1.9661423534	-4.1984423378
C	6.0	-9.3448788377	1.9661423534	-4.1984423378

C	6.0	10.2384239276	0.6767512222	-3.7677842839
C	6.0	-10.2384239276	-0.6767512222	-3.7677842839
C	6.0	10.4621530752	-1.4983519416	-4.8321422870
C	6.0	-10.4621530752	1.4983519416	-4.8321422870
C	6.0	10.9152979653	-0.1566388999	-4.6141146723
C	6.0	-10.9152979653	0.1566388999	-4.6141146723
H	1.0	0.0300873284	-1.0629347928	5.7788949145
H	1.0	-0.0300873284	1.0629347928	5.7788949145
H	1.0	0.4960165662	-3.3192073619	2.7796139388
H	1.0	-0.4960165662	3.3192073619	2.7796139388
H	1.0	0.5424541299	-4.0938497009	4.3751290942
H	1.0	-0.5424541299	4.0938497009	4.3751290942
H	1.0	0.8383584030	4.3601034903	3.2934822506
H	1.0	-0.8383584030	-4.3601034903	3.2934822506
H	1.0	1.0520129262	3.3429443421	6.2271145789
H	1.0	-1.0520129262	-3.3429443421	6.2271145789
H	1.0	1.2211522491	-1.6638920328	4.6399512493
H	1.0	-1.2211522491	1.6638920328	4.6399512493
H	1.0	1.5114831911	-1.4865271168	1.9101780592
H	1.0	-1.5114831911	1.4865271168	1.9101780592
H	1.0	2.2215779806	2.0409150799	5.9257571001
H	1.0	-2.2215779806	-2.0409150799	5.9257571001
H	1.0	2.4284692981	3.6175344304	5.1447006516
H	1.0	-2.4284692981	-3.6175344304	5.1447006516
H	1.0	3.1365631204	3.1748093057	2.7467203793
H	1.0	-3.1365631204	-3.1748093057	2.7467203793
H	1.0	3.3629779909	-1.8343543054	0.3252806125
H	1.0	-3.3629779909	1.8343543054	0.3252806125
H	1.0	4.3810200476	-4.6752997674	-1.6750627420

H	1.0	-4.3810200476	4.6752997674	-1.6750627420
H	1.0	4.9693291334	2.8077689791	1.1307670675
H	1.0	-4.9693291334	-2.8077689791	1.1307670675
H	1.0	7.1148626140	-2.5899925977	-2.8066501798
H	1.0	-7.1148626140	2.5899925977	-2.8066501798
H	1.0	7.6666362263	4.9161475464	-0.0549336149
H	1.0	-7.6666362263	-4.9161475464	-0.0549336149
H	1.0	8.6976894303	2.0673781211	-2.0389535753
H	1.0	-8.6976894303	-2.0673781211	-2.0389535753
H	1.0	8.9978422327	-2.9838589492	-4.3619818407
H	1.0	-8.9978422327	2.9838589492	-4.3619818407
H	1.0	10.5802690802	1.6956178076	-3.6002803224
H	1.0	-10.5802690802	-1.6956178076	-3.6002803224
H	1.0	11.0172091321	-2.1427894290	-5.5089136131
H	1.0	-11.0172091321	2.1427894290	-5.5089136131
H	1.0	11.8054106577	0.1938997995	-5.1301113717
H	1.0	-11.8054106577	-0.1938997995	-5.1301113717

BCO

ATOM	CHARGE	X	Y	Z
C	6.0	-0.4764452138	1.3397132137	0.2536152070
C	6.0	0.4764452138	-1.3397132137	0.2536152070
C	6.0	-0.7345639418	0.2524027509	-1.9968906675
C	6.0	0.7345639418	-0.2524027509	-1.9968906675
C	6.0	-1.0480404916	-1.0784608407	0.0949495468
C	6.0	1.0480404916	1.0784608407	0.0949495468
C	6.0	-1.3055509798	0.3013155450	-0.5506262803
C	6.0	1.3055509798	-0.3013155450	-0.5506262803
C	6.0	-2.7839336638	0.6894654286	-0.5882680072
C	6.0	2.7839336638	-0.6894654286	-0.5882680072
C	6.0	-3.1556719480	1.9599880606	-1.1666000064
C	6.0	3.1556719480	-1.9599880606	-1.1666000064
C	6.0	-3.7895024031	-0.1194392009	-0.1229464259
C	6.0	3.7895024031	0.1194392009	-0.1229464259
C	6.0	-4.4556678812	2.3626079483	-1.2595161115
C	6.0	4.4556678812	-2.3626079483	-1.2595161115
C	6.0	-5.1732678437	0.2574443937	-0.1939697638
C	6.0	5.1732678437	-0.2574443937	-0.1939697638
C	6.0	-5.5222908380	1.5332263411	-0.7813298935
C	6.0	5.5222908380	-1.5332263411	-0.7813298935
C	6.0	-6.1876101410	-0.5672537590	0.2794128624
C	6.0	6.1876101410	0.5672537590	0.2794128624
C	6.0	-6.8576399378	1.9060706446	-0.8654873266
C	6.0	6.8576399378	-1.9060706446	-0.8654873266
C	6.0	-7.5506840538	-0.2032157255	0.2013977206
C	6.0	7.5506840538	0.2032157255	0.2013977206

C	6.0	-7.8980217143	1.0750507335	-0.3937149134
C	6.0	7.8980217143	-1.0750507335	-0.3937149134
C	6.0	-7.9561632947	-3.3747601143	1.7729492577
C	6.0	7.9561632947	3.3747601143	1.7729492577
C	6.0	-8.2433301938	-2.3077397712	1.2736641584
C	6.0	8.2433301938	2.3077397712	1.2736641584
C	6.0	-8.5815028050	-1.0551559507	0.6867655109
C	6.0	8.5815028050	1.0551559507	0.6867655109
C	6.0	-9.2637934527	1.4600272086	-0.4911265731
C	6.0	9.2637934527	-1.4600272086	-0.4911265731
C	6.0	-9.6028822167	2.7143332201	-1.0739733800
C	6.0	9.6028822167	-2.7143332201	-1.0739733800
C	6.0	-9.8923478095	3.7825853721	-1.5691909036
C	6.0	9.8923478095	-3.7825853721	-1.5691909036
C	6.0	-9.9487317964	-0.6702085902	0.5899353194
C	6.0	9.9487317964	0.6702085902	0.5899353194
C	6.0	-10.2955228121	0.6043505331	-0.0125710251
C	6.0	10.2955228121	-0.6043505331	-0.0125710251
C	6.0	-10.9881409626	-1.4992754256	1.0648354240
C	6.0	10.9881409626	1.4992754256	1.0648354240
C	6.0	-11.6582553743	0.9605845019	-0.1077274844
C	6.0	11.6582553743	-0.9605845019	-0.1077274844
C	6.0	-12.3272129805	-1.1366239320	0.9678013713
C	6.0	12.3272129805	1.1366239320	0.9678013713
C	6.0	-12.6736179419	0.1329307825	0.3587362267
C	6.0	12.6736179419	-0.1329307825	0.3587362267
C	6.0	-13.3853444936	-1.9775515445	1.4489347692
C	6.0	13.3853444936	1.9775515445	1.4489347692
C	6.0	-14.0592663701	0.4909154347	0.2588419046

C	6.0	14.0592663701	-0.4909154347	0.2588419046
C	6.0	-14.6925918767	-1.5953574571	1.3339017959
C	6.0	14.6925918767	1.5953574571	1.3339017959
C	6.0	-15.0347877481	-0.3430490865	0.7285747672
C	6.0	15.0347877481	0.3430490865	0.7285747672
H	1.0	-0.7179708944	2.3577509153	-0.0704453676
H	1.0	0.7179708944	-2.3577509153	-0.0704453676
H	1.0	-0.7714948832	1.2791460190	1.3086967220
H	1.0	0.7714948832	-1.2791460190	1.3086967220
H	1.0	-0.7918214789	1.2522137316	-2.4424566273
H	1.0	0.7918214789	-1.2522137316	-2.4424566273
H	1.0	-1.3670846154	-0.3975431498	-2.6131437079
H	1.0	1.3670846154	0.3975431498	-2.6131437079
H	1.0	-1.5324440838	-1.1316996351	1.0767966399
H	1.0	1.5324440838	1.1316996351	1.0767966399
H	1.0	-1.5058276820	-1.8597022783	-0.5252825445
H	1.0	1.5058276820	1.8597022783	-0.5252825445
H	1.0	-2.3761655540	2.6155032773	-1.5437853227
H	1.0	2.3761655540	-2.6155032773	-1.5437853227
H	1.0	-3.5664432568	-1.0866591109	0.3158820338
H	1.0	3.5664432568	1.0866591109	0.3158820338
H	1.0	-4.7047769571	3.3236869894	-1.7037279543
H	1.0	4.7047769571	-3.3236869894	-1.7037279543
H	1.0	-5.9315414927	-1.5242823697	0.7237827363
H	1.0	5.9315414927	1.5242823697	0.7237827363
H	1.0	-7.1177598128	2.8620043498	-1.3097332167
H	1.0	7.1177598128	-2.8620043498	-1.3097332167
H	1.0	-7.7040260524	-4.3131791310	2.2128073222
H	1.0	7.7040260524	4.3131791310	2.2128073222

H	1.0	-10.1475684010	4.7226687179	-2.0037050719
H	1.0	10.1475684010	-4.7226687179	-2.0037050719
H	1.0	-10.7261450366	-2.4498957806	1.5192256846
H	1.0	10.7261450366	2.4498957806	1.5192256846
H	1.0	-11.9153898183	1.9121142101	-0.5630411043
H	1.0	11.9153898183	-1.9121142101	-0.5630411043
H	1.0	-13.1219401696	-2.9275378423	1.9081342459
H	1.0	13.1219401696	2.9275378423	1.9081342459
H	1.0	-14.3151864759	1.4424779022	-0.2013173717
H	1.0	14.3151864759	-1.4424779022	-0.2013173717
H	1.0	-15.4856162601	-2.2413602955	1.7013990838
H	1.0	15.4856162601	2.2413602955	1.7013990838
H	1.0	-16.0812316166	-0.0609211682	0.6467967405
H	1.0	16.0812316166	0.0609211682	0.6467967405

BP1

ATOM	CHARGE	X	Y	Z
C	6.0	-8.0485818451	-3.7237053082	0.0054647754
C	6.0	8.0485818451	3.7237053082	-0.0054647754
C	6.0	-9.8250290768	4.2132293761	-0.0462643742
C	6.0	9.8250290768	-4.2132293761	0.0462643742
C	6.0	-8.3137023579	-2.5404745836	-0.0005506411
C	6.0	8.3137023579	2.5404745836	0.0005506411
C	6.0	-9.5609933304	3.0298913551	-0.0361403395
C	6.0	9.5609933304	-3.0298913551	0.0361403395
C	6.0	-2.7784242015	0.8565068231	-0.0106152265
C	6.0	2.7784242015	-0.8565068231	0.0106152265
C	6.0	-8.6251628900	-1.1510801680	-0.0070831675
C	6.0	8.6251628900	1.1510801680	0.0070831675
C	6.0	-3.8052461148	-0.0591692138	-0.0061368347
C	6.0	3.8052461148	0.0591692138	0.0061368347
C	6.0	-13.4569436451	-2.2159620862	0.0310623573
C	6.0	13.4569436451	2.2159620862	-0.0310623573
C	6.0	-11.0459118923	-1.6660373497	0.0091673069
C	6.0	11.0459118923	1.6660373497	-0.0091673069
C	6.0	-1.3606844358	0.4252068193	0.0010867843
C	6.0	1.3606844358	-0.4252068193	-0.0010867843
C	6.0	-3.1110848312	2.2611074569	-0.0309948293
C	6.0	3.1110848312	-2.2611074569	0.0309948293
C	6.0	-9.2495747155	1.6402805396	-0.0249065538
C	6.0	9.2495747155	-1.6402805396	0.0249065538
C	6.0	-9.9854544125	-0.7344534775	-0.0038226767
C	6.0	9.9854544125	0.7344534775	0.0038226767

C	6.0	-6.2167907364	-0.5858801703	-0.0116434413
C	6.0	6.2167907364	0.5858801703	0.0116434413
C	6.0	-5.1787720204	0.3400827270	-0.0140310598
C	6.0	5.1787720204	-0.3400827270	0.0140310598
C	6.0	-7.5725372462	-0.1937629842	-0.0154451965
C	6.0	7.5725372462	0.1937629842	0.0154451965
C	6.0	-12.3785996776	-1.2700893786	0.0157137741
C	6.0	12.3785996776	1.2700893786	-0.0157137741
C	6.0	-14.7575273915	-1.7967498923	0.0384261298
C	6.0	14.7575273915	1.7967498923	-0.0384261298
C	6.0	-7.8898670648	1.2237967054	-0.0250531840
C	6.0	7.8898670648	-1.2237967054	0.0250531840
C	6.0	-10.3032215268	0.6826172482	-0.0120240412
C	6.0	10.3032215268	-0.6826172482	0.0120240412
C	6.0	-5.4961436860	1.7540665160	-0.0300554604
C	6.0	5.4961436860	-1.7540665160	0.0300554604
C	6.0	-6.8262074665	2.1543863764	-0.0338978468
C	6.0	6.8262074665	-2.1543863764	0.0338978468
C	6.0	-4.4069982394	2.6874055869	-0.0380689613
C	6.0	4.4069982394	-2.6874055869	0.0380689613
C	6.0	-11.6600499417	1.0722947090	-0.0061844547
C	6.0	11.6600499417	-1.0722947090	0.0061844547
C	6.0	-12.6965807431	0.1450900556	0.0080110090
C	6.0	12.6965807431	-0.1450900556	-0.0080110090
C	6.0	-15.0719988454	-0.3990386787	0.0304458487
C	6.0	15.0719988454	0.3990386787	-0.0304458487
C	6.0	-14.0764305448	0.5374840655	0.0156705008
C	6.0	14.0764305448	-0.5374840655	-0.0156705008
C	6.0	-0.9517099938	-0.7174274363	0.7118461078

C	6.0	0.9517099938	0.7174274363	-0.7118461078
C	6.0	-0.3748225516	1.1355201328	-0.7068700352
C	6.0	0.3748225516	-1.1355201328	0.7068700352
H	1.0	-7.8167017117	-4.7648659902	0.0091748498
H	1.0	7.8167017117	4.7648659902	-0.0091748498
H	1.0	-10.0576983520	5.2541615055	-0.0544416670
H	1.0	10.0576983520	-5.2541615055	0.0544416670
H	1.0	-13.2147320505	-3.2762272297	0.0367075555
H	1.0	13.2147320505	3.2762272297	-0.0367075555
H	1.0	-10.8069851067	-2.7251804449	0.0151348524
H	1.0	10.8069851067	2.7251804449	-0.0151348524
H	1.0	-3.5860159263	-1.1238792552	-0.0245189921
H	1.0	3.5860159263	1.1238792552	0.0245189921
H	1.0	-15.5659637783	-2.5231270509	0.0501461824
H	1.0	15.5659637783	2.5231270509	-0.0501461824
H	1.0	-2.3052031116	2.9892256686	-0.0097159598
H	1.0	2.3052031116	-2.9892256686	0.0097159598
H	1.0	-5.9844889410	-1.6463750690	-0.0031890392
H	1.0	5.9844889410	1.6463750690	0.0031890392
H	1.0	-7.0628761999	3.2140711377	-0.0427747401
H	1.0	7.0628761999	-3.2140711377	0.0427747401
H	1.0	-4.6356497773	3.7507431995	-0.0390566355
H	1.0	4.6356497773	-3.7507431995	0.0390566355
H	1.0	-11.8941664546	2.1325428491	-0.0119206856
H	1.0	11.8941664546	-2.1325428491	0.0119206856
H	1.0	-16.1138049044	-0.0896529288	0.0368014893
H	1.0	16.1138049044	0.0896529288	-0.0368014893
H	1.0	-14.3116948967	1.5993440797	0.0101576338
H	1.0	14.3116948967	-1.5993440797	-0.0101576338

H	1.0	-1.6795156218	-1.2663093410	1.3030606966
H	1.0	1.6795156218	1.2663093410	-1.3030606966
H	1.0	-0.6574102132	2.0047748622	-1.2948540577
H	1.0	0.6574102132	-2.0047748622	1.2948540577